03 May 2013, 1:45 pm - 2:05 pm

A Report on the 2012 Seismic Sequence in Emilia (Northern Italy)

Diego C. F. Lo Presti
University of Pisa, Italy

Mauro Sassu
University of Pisa, Italy

Lucia Luzi
INGV Sezione di Milano, Italy

Francesca Pacor
INGV Sezione di Milano, Italy

Doriano Castaldini
University of Modena and Reggio Emilia, Italy

Diego C. F. Lo Presti, Mauro Sassu, Lucia Luzi, Francesca Pacor, Doriano Castaldini, Giovanni Tosatti, Claudia Meisina, Davide Zizioli, Francesco Zucca, Giuliano Rossi, Gilberto Saccorotti, and Davide Piccinini

Commemorate the Legacy of Ralph B. Peck
April 29 - May 4, 2013 CHICAGO
Seventh International Conference on Case Histories in Geotechnical Engineering
and Symposium in Honor of Clyde Baker

A REPORT ON THE 2012 SEISMIC SEQUENCE IN EMILIA (NORTHERN ITALY)

Diego C. F. Lo Presti, & Mauro Sassu
University of Pisa, Department of Civil Engineering, Largo Lucio Lazzarino, 1- Pisa, Italy, 56122, Italy, d.lopresti@ing.unipi.it , tel: +39 050 2217742, fax: +39 050 2217762
Lucia Luzi & Francesca Pacor
INGV Sezione di Milano – Pavia, via Bassini 15, 20133 Milano, lucia.luzi@mi.ingv.it, tel. +39 02 23699280, fax +39 02 23699267
Doriano Castaldini & Giovanni Tosatti
University of Modena and Reggio Emilia, Department of Chemical and Geological Sciences, Largo S. Eufemia 19, 41100 Modena, doriano.castaldini@unimore.it, tel. +39 059 2055856, fax +39 059 2055887
Claudia Meisina, Davide Zizioli & Francesco Zucca
University of Pavia, Department of Earth & Environmental Sciences, via Ferrata 1 27100 Pavia, claudia.meisina@unipv.it, tel. +39 0382 985831
Giuliano Rossi
Provincia di Mantova, Progettazione della Viabilità e delle Infrastrutture, Via Principe Amedeo n. 32, Mantova giuliano.rossi@provincia.mantova.it, tel. ++390376 204285
Gilberto Saccorotti & Davide Piccinini
INGV – Sezione di Pisa Via U. della Faggiola, 32 – 56126 PISA (I) tel +39 050 8311960 saccorotti@pi.ingv.it

ABSTRACT

Since mid-May 2012, an energetic seismic sequence has affected the northern part of Italy and specifically a wide sector of the Po River Plain. The sequence has been dominated by two main events: a) Mw = 5.9 occurred near Finale Emilia on May 20th at a depth of 6.3 km, and b) Mw=5.8 occurred near Cavezzo on May 29th at a depth of 10.2 km (earthquake location are obtained Istituto Nazionale di Geofisica e Vulcanologia, http://iside.rm.ingv.it/). The effects of the two main shocks can be summarized as follows:

- damage to infrastructures (roads, pipelines) essentially because of the occurrence of liquefaction phenomena or soil failure;
- damage to very old constructions (especially churches and bell towers – masonry and brickworks);
- recent constructions such as barns and industrial premises have collapsed. These constructions were mainly isostatic structures not designed to withstand earthquakes.

The paper deals with the following arguments:

- seismological aspects, mainly related to the seismo - tectonic framework, the source mechanisms, and the comparison between the observed seismic motion and that expected on the basis of the National Map of Seismic Hazard;
- identification and mapping of the soil failures (liquefaction) and induced damage with special emphasis on the geomorphologic structures showing the presence of ancient riverbeds;
- description of the structural damage regarding the historical buildings and the modern industrial buildings.

In conclusion the report will try to explain the reasons for the large damage observed in the case of both ancient and modern constructions.

INTRODUCTION

Since mid-May May 2012, an energetic seismic sequence is interesting the northern part of Italy and specifically a wide sector of the River Po Plain pertaining to the Emilia Romagna Region. The sequence was preceded by a few foreshocks, the most energetic of which was a ML = 4.1 on May 19th, 2012. Thus far, the sequence has been dominated by two main events, namely a) Mw = 5.9 occurred near Finale Emilia on May 20th at a depth of 6.3 km, and b) Mw = 5.8 occurred near Cavezzo on May 29th at a depth of 10.2 km. During the first two weeks of the sequence 7 earthquakes with magnitude larger than 5 occurred. By the time of writing this note (early September, 2012) the catalogue from the national monitoring system, ISIDe (http://iside.rm.ingv.it/) by the Istituto Nazionale di Geofisica e Vulcanologia (INGV hereinafter), accounts for more than 2,500 locations, with a completeness magnitude around 2.

The effects of the two main shocks are summarized as follows:
- 27 lives were lost, hundreds of persons were injured and at least 40,000 people were evacuated;
- damage to infrastructures (roads, pipelines) essentially because of the occurrence of liquefaction phenomena or soil failures;
- damage to very old constructions (especially churches, bell towers and masonry and brickwork);
- as for the very recent constructions, many barns and industrial premises have shown a dramatic collapse. These constructions were mainly isostatic structures not designed to withstand earthquakes. In addition, relevant non - structural features were strongly damaged.
- economic losses of some 2 billion euros.

A special issue on the preliminary data and results of the Emilia seismic sequence was published by Anzidei et al. (2012).

In particular, the following topics are dealt with:-
- seismological aspects referring mainly to the focal mechanisms and the level of the seismic motion in comparison with the prescription of the Italian Building Code;
- identification and mapping of the soil failures (liquefaction) and induced damage, with special emphasis on the geomorphologic structures showing the presence of ancient riverbeds;
- description of the structural damages regarding the historical building and the modern industrial buildings.

SEISMOLOGICAL ASPECTS

Tectonics of the area

The seismic sequence object of this paper developed along the Northern Apennines frontal thrust system, which is constituted by a pile of NE-verging tectonic units that formed as a consequence of Cenozoic collision between the European and the Adria plates (Boccaletti *et al.* 2011; see Fig. 1). This thrust front is covered by a thick (less than 100 meters to 8 km) Plio-Pleistocenic sedimentary deposits of fluvial origin. Nonetheless, geometry and location of the main faults are now well established, thanks to extensive seismic reflection surveys conducted during the 70's for oil and gas exploration (Ori and Friend, 1984). Present-day, active NE-SW compression throughout the outer Apennines front and Po plain is documented by GPS data, that show an average horizontal shortening of approximately 1 mm/y (Zerbini *et al.*, 2006), and by both borehole breakouts data (Montone *et al.*, 2004) and centroid moment tensor solutions of large (Mw > 4) earthquakes (Pondrelli *et al.* 2006).

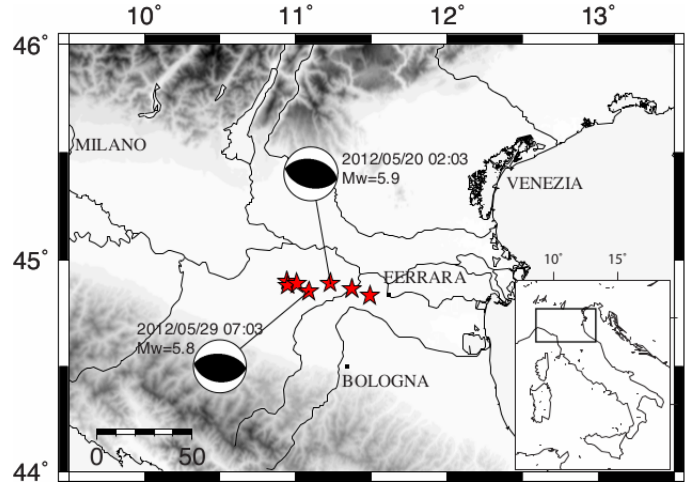

Fig. 1. – Map of Northern Italy reporting the location of the strongest (Mw > 5) earthquakes of the 2012 sequence (red stars). The two mainshocks have attached the focal solution, and are labeled by the corresponding origin time and moment magnitude. Main cities are labeled.

The seismic sequence and historical seismicity

The seismic sequence began on 2012 May 20th (02:03:53 UTC), with a Mw 5.86 (ML 5.9) earthquake. This mainshock was preceded, a few hours before, by a Mw 3.98 (ML 4.1) foreshock, almost co-located with the main event. Within the following 15 days, the seismic sequence included six additional earthquakes with magnitude greater than 5.0 (see Fig. 1). The most energetic of these, located about 12 km west of the May 20th mainshock, was a Mw 5.66 (ML 5.8) on May 29th (07:00:03 UTC). By the time of writing this paper (early September, 2012), the sequence is gradually waning (Fig.2).

The two most energetic events, similarly to other large shocks of the sequence, exhibit a focal mechanism consistent with the activation of EW-striking thrust faults, as indicated by time domain moment tensor solutions (TDMT) routinely calculated using optimal subsets of INGV's national seismic network (Scognamiglio *et al.*, 2009; Fig. 1), and in agreement with the tectonic setting and active stress field of the area. Preliminary analyses of the May 20th mainshock (Piccinini *et al.*, 2012) indicate that this event was constituted by at least three distinct sub-events, likely related to multi-lateral rupture propagation toward the eastern and western tips of the fault plane. The May 29th, Mw=5.8 event occurred about 12 km WSW of the May 20th mainshock activating an adjacent fault segment. At present, the geometrical relationships between the structures activated by these two main events are still to be clarified.

Epicenters extend approximately 50 km along the EW direction; the hypocentral depths span the 0-40 km depth interval, with the large majority of hypocenters concentrated within the shallowest 10 km of crust. Although these catalog locations do not allow for a clear identification of the geometries of the activated structures, a NS cross-section delineates a plane dipping South by about 45° (Fig. 3, bottom), which is consistent with one of the focal planes obtained from moment tensor inversion of the most energetic shocks (Fig 1) and with the inferred setting of the thrust front. These data thus confirm that the current activity of Northern Apennines thrust systems is controlled by an overall North – South oriented compressive stress field acting on EW-striking, S-dipping buried thrust faults.

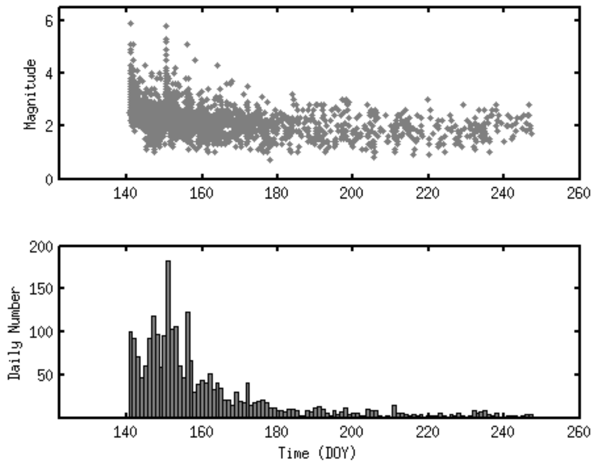

Fig. 2 – Temporal evolution of sequence, in terms of Magnitude (top) and daily number of earthquakes (bottom) versus time. The time scale is in day-of-the-year; for reference, day 140 is May 19th, 2012.

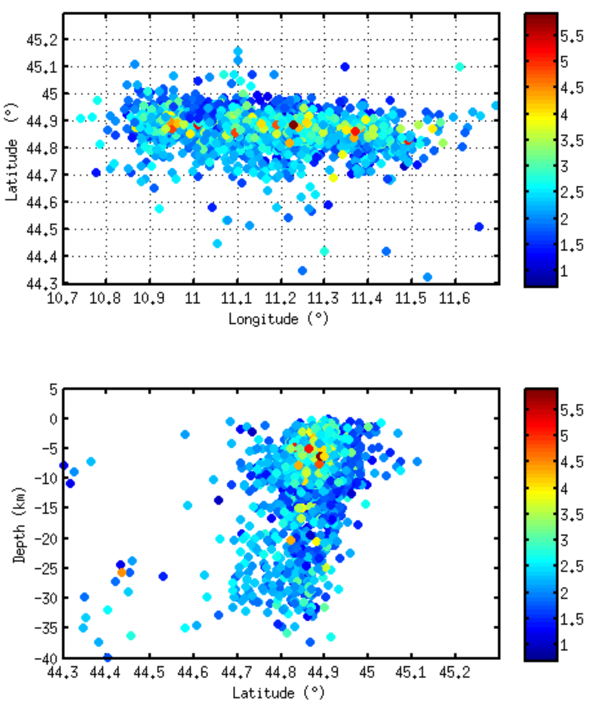

Fig. 3 – Hypocentral distribution in map view (top) and projected onto a NS cross-section (bottom). Color is proportional to magnitude, according to the color scale at the right.

Both historical (Rovida *et al.*, 2011) and instrumental catalogues (ISIDE database: http://iside.rm.ingv.it) indicate that the seismicity rate for this sector of the Po Plain is lower than that characterizing the Northern Apennines belt. The most important historical event is the Mw = 5.5 earthquake which, on late 1570, struck the city of Ferrara. This shock was followed by a complex series of aftershocks, lasting till early 1572. For the 1570 main-shock, historical reports document liquefaction effects (Galli, 2000).

Response Spectra and seismic response analyses

The strong motion data have been obtained from the permanent and temporary stations of the Italian strong motion network managed by the Department of Civil Protection (DPC, www.protezionecivile.gov.it). Additional data have been obtained from the network managed by INGV.

Table 1 Strong motion stations and parameters of the Italian Building Code NTC (2008) for the response spectra: STA = station code; LA_ST = station latitude; LO_ST = station longitude; EC8 = EC8 class; Network = recording network (IT = DPC); the two series of values a_g F_0 and T*c are the parameters of NTC (2008) for return periods of 475 and 975 years, respectively.

STA	LA_ST	LO_ST	EC8	Network	Ag (g)	F_0	T*c (s)	Ag (g)	F_0	T*c (s)
SMS0	44.934	11.235	C*	IT	0.120	2.590	0.279	0.161	2.565	0.283
MRN	44.878	11.062	C*	IT	0.140	2.588	0.269	0.193	2.538	0.276
SAN0	44.838	11.143	C*	IT	0.150	2.588	0.269	0.202	2.537	0.276
MOG0	44.932	10.912	C*	IT	0.123	2.580	0.276	0.166	2.555	0.278
FIN0	44.829	11.286	C*	IT	0.150	2.588	0.270	0.202	2.537	0.277
RAV0	44.715	11.142	C*	IT	0.157	2.591	0.273	0.210	2.527	0.280

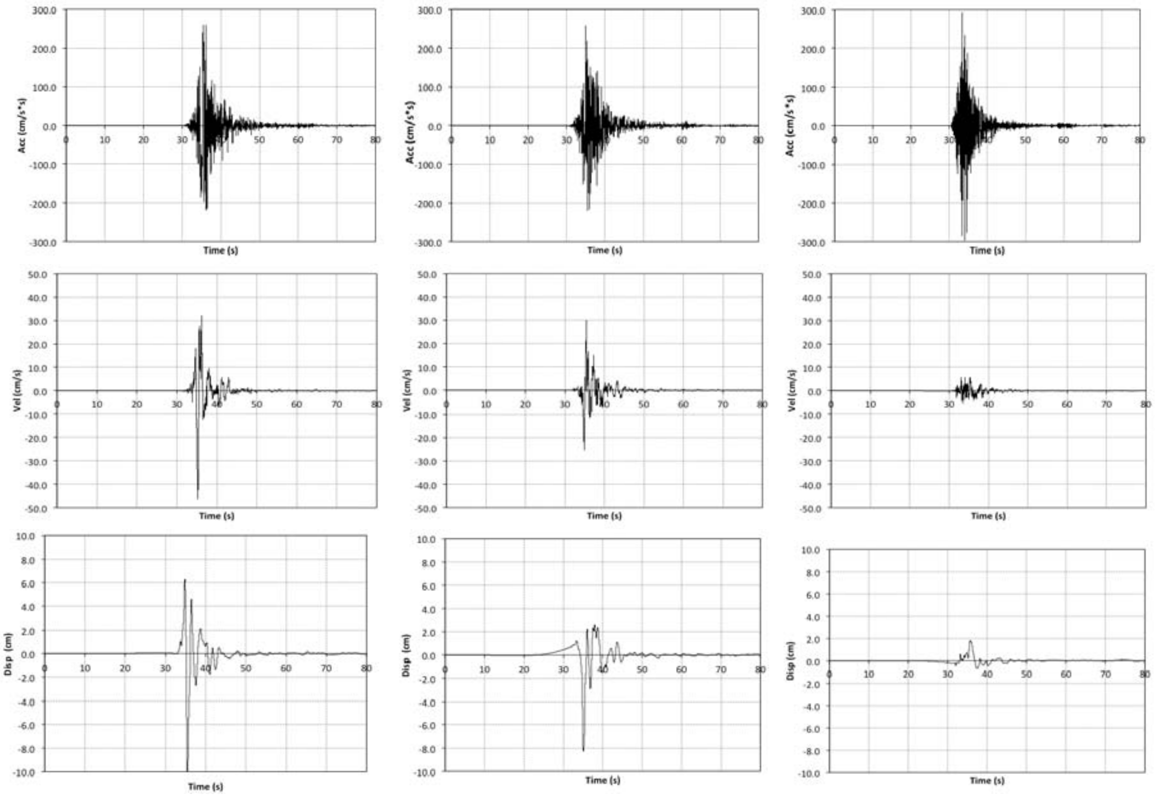

Fig. 4: Acceleration (top panel), velocity (central panel) and displacement (bottom panel) recorded at Mirandola (MRN) during May 20th (left NS, centre EW and right UP components)

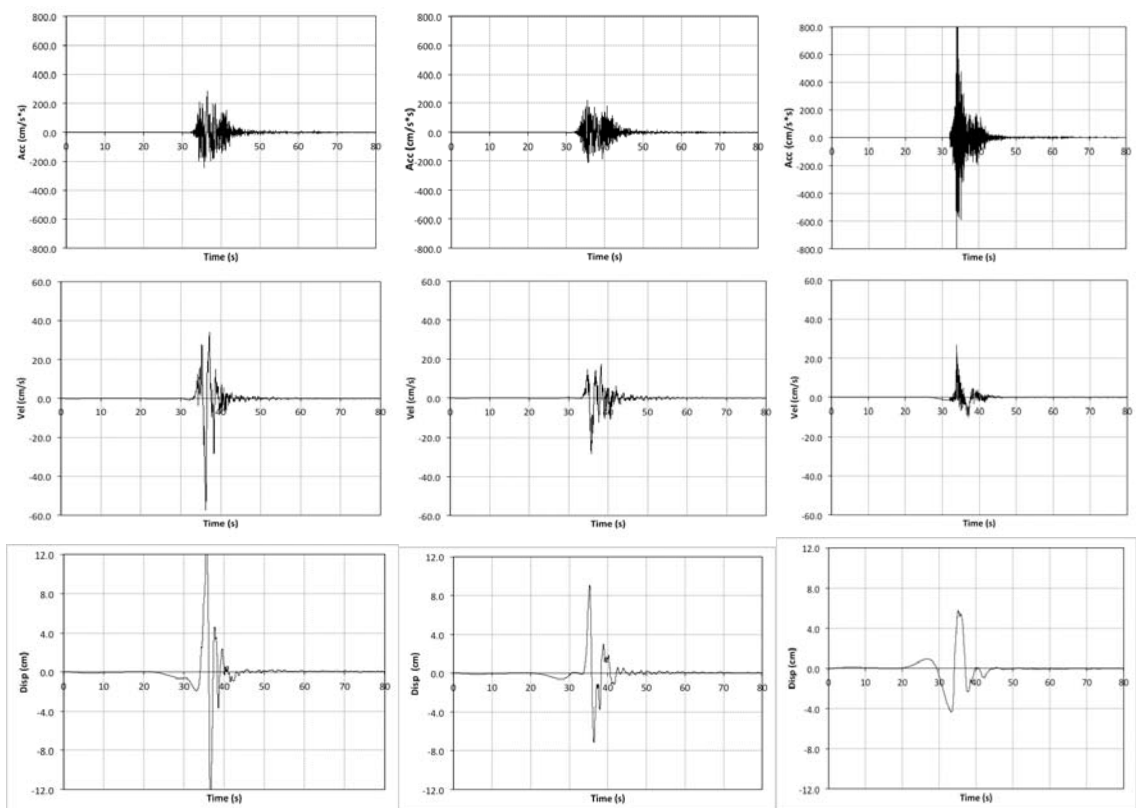

Fig. 5: Acceleration (top panel), velocity (central panel) and displacement (bottom panel) recorded at Mirandola (MRN) during May 29th (left NS, centre EW and right UP components)

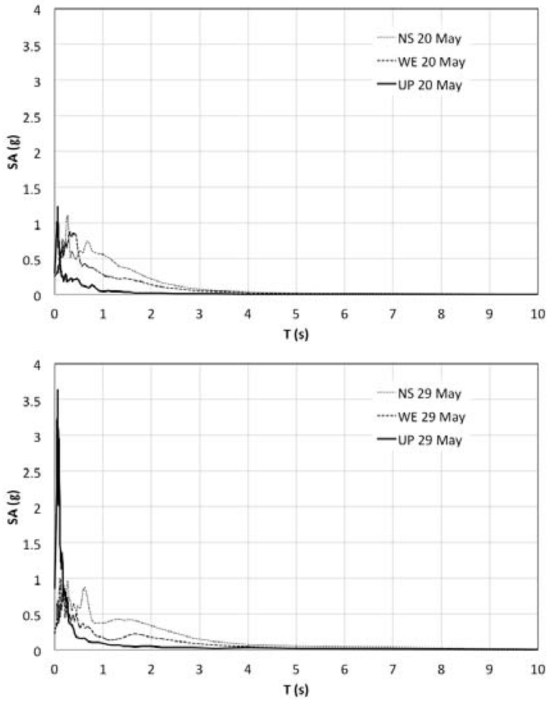

Fig. 6: Left spectral acceleration at MRN during May 20th; right spectral acceleration at MRN during May 29th.

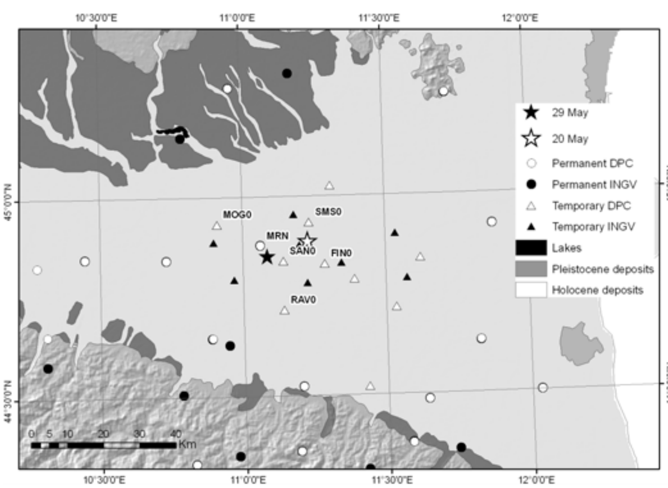

Fig. 7. Map of the station installed by the DPC and INGV

The recorded waveforms have been processed adopting the procedure described in Pacor *et al*. (2011). This method includes the removal of the linear trend fitting the entire record, a cosine taper, and the application of a time-domain acausal 4th-order Butterworth band-pass filter. Before executing the filtering procedure zero pads are added, as in Boore and Bommer (2005). Both the high-pass and low-pass frequencies are selected through visual inspection of the Fourier spectrum. The typical band-pass frequency range is between 0.08 and 40 Hz. Zero pads are then removed from the filtered signal and a procedure is applied in order to guarantee the compatibility between acceleration velocity and displacement by subsequent integration.

Figures 4 and 5 display the acceleration, velocity and displacement time series of the two strongest shocks recorded at the station Mirandola (MRN). The vertical component of the motion, for both shocks is characterized by strong energy content at high frequencies and, as a consequence, the vertical PGA is larger than the two horizontal components. At decreasing frequencies the energy is mainly carried by the horizontal components, especially by the NS component, which is approximately normal to the fault strike. The acceleration spectral amplitudes at different periods are shown in Fig. 6, for the strongest shocks as recorded at the Mirandola, Station.

The acceleration response spectra, that have been computed from the records of stations with epicentral distances ranging from 3.5 to 16 km, were compared to the uniform hazard spectra of the NTC (2008) (5% damping) considering return periods of 475 and 975 years, respectively. The parameters for computing the uniform hazard acceleration response spectra are given by CSLP (2012) (see also Table 1).

It is worthwhile to report the equations prescribed by the Italian Building Code (NTC 2008) for the uniform – hazard horizontal elastic acceleration response spectra.

$$S_e(T) = a_g S \cdot \eta \cdot F_o \left(\frac{T}{T_B} + \frac{(1 - T/T_B)}{\eta \cdot F_o} \right) \quad (1)$$

$$S_e(T) = a_g S \cdot \eta \cdot F_o \quad (2)$$

$$S_e(T) = a_g S \cdot \eta \cdot F_o \left(\frac{T_C}{T} \right) \quad (3)$$

$$S_e(T) = a_g S \cdot \eta \cdot F_o \left(\frac{T_C T_D}{T^2} \right) \quad (4)$$

Where: $\eta = \sqrt{10/(5+\xi)} \geq 0.55$ takes into account values of the structural damping ratio different than the conventional ξ = 5%; $S_e(T)$ is the elastic acceleration spectral ordinate and T is the vibration period; S takes into account both stratigraphic and topographic amplification in a way similar to that prescribed by Eurocode 8 (2004) (for NTC 2008 the stratigraphic amplification factor depends on soil category, PGA on rock soil and on the parameter F_o); $F_o > 2.2$ represents the maximum spectral amplification and is a site dependent parameter (see Table 1); $T_c = C_c \cdot T_c^*$ is the period beyond which spectral velocity is constant (this parameter is site dependent by the effect of T_c^* as shown in Table 1 and also depends on soil category by the effect of C_c); $T_B = T_c / 3$ is the period beyond which the spectral acceleration is constant; $T_D = 4 \cdot a_g + 1.6$ is the period beyond which the spectral displacement is constant; a_g is the PGA on rock soil.

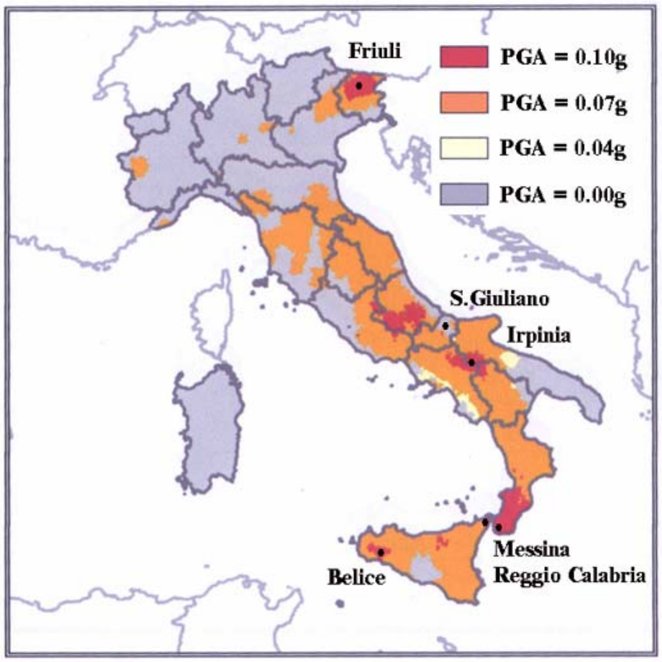

Fig. 8. Seismic macrozonation map of Italy before 2003.

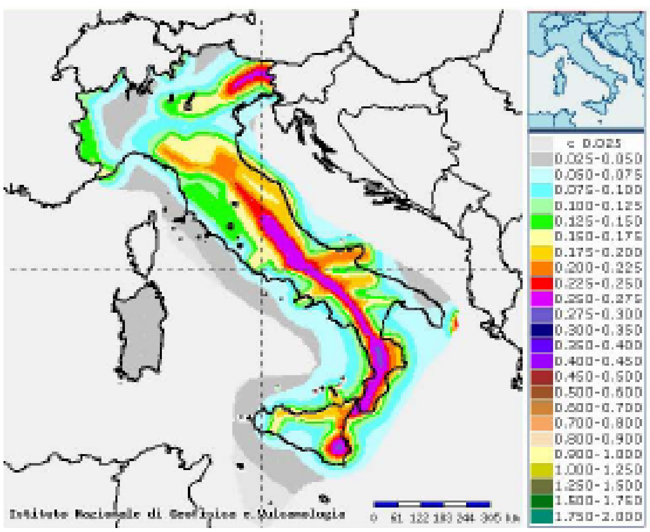

Fig.9. Seismic macrozonation map of Italy for a return period of 475 years based on a probabilistic approach after 2010.

PGA have been computed following a probabilistic approach at the apex of a square grid of 0.05° length for different return periods by INGV (http://zonesismiche.mi.ingv.it; http://esse1.mi.ingv.it/) 2012 – updated version). Figures 8-9 compare the hazard maps for the Italian territory before 2003 and after 2010.

This hazard map became mandatory after 2006 (G.U. n.108 del 11/05/2006). The Italian seismic code (NTC08), which prescribes the seismic actions according to the outcomes of the probabilistic studies, is mandatory since December 2009. The obligation for retrofitting of existing building is mandatory only for the so – called "strategic" structures (Hospitals, Fire-brigade buildings etc. i.e. any building and infrastructure fundamental for the civil service).

Six stations have been selected close to the fault, in particular Mirandola (MRN) that recorded both the shocks of May 20 and May 29 and five temporary stations (SAN0, MOG0, FIN0, RAV0, SMS0), shown in Fig. 7. The comparison is shown in Figures from 10a to 10f. Although the comparison of observations with response spectra has few significance, as the probabilistic outcomes are compared to one single event, in general the agreement between observations and the code spectra are very good. The most evident Some discrepancies arecan be observed for periods longer than 1 s and very close to the fault (station SAN0 and MRN, Figures 10a and 10b), or NW of the epicentre (station MOG0, Figure 10d), where the observations exceed both the spectra for a return period of 475 and 975 years. This effect can be probably ascribed to source effects of the event of May 29th. The spectral ordinates recorded to the south (station RAV0, Figure 10e) are below the ones prescribed by the Italian code.

The attenuation with distance and magnitude scaling of the peak ground motion parameters, PGA and PGV, and the acceleration spectral ordinates (5% damping) at different periods, observed on May 29th, have been compared to the values inferred from ground motion prediction equations (GMPE) of the ITA10 (Bindi *et al.*, 2011), recently derived from a qualified data set almost entirely consisting of crustal events recorded in the central – southern Apennines. For the comparison reverse fault mechanism and appropriate site conditions are assumed. Due to the scarce information about local site conditions, the observations were grouped into two classes: soft sites (EC8 class C, grey circles, for a comparison with ITA10 class C) and rock and stiff soil (EC8 class A and B, black circles, for a comparison with ITA10 class A).

The comparison with ITA10 of the geometric mean of the horizontal components up to 200 km (Figures 11a - 11b) indicates that, in general, the agreement between observations and predictions is good with few exceptions. In particular, the observed PGAs and PGVs decay faster than ITA10 at distances larger than 100 km, where several points fall below the median minus one standard deviation. At distances less than 10 km, observed PGAs are within the mean minus one standard deviation, while the opposite in observed for PGVs that are within one standard deviation above the mean. Figures 9c and 9d show the vertical PGAs and PGVs compared to the ITA10: the mean predictions for EC8 C site well fit the observed PGAs, except for one record observed above the fault (station MRN) that is strongly underestimated by the model. In terms of vertical PGV, the ITA10 predictions for EC8 C sites overestimate the observed peak values that decay with distance similarly to the mean for EC8 A sites. These trends suggest that, in the proximity of the source, the high frequency of the vertical motion is much larger than the Italian mean, although the decay is faster, as also observed for the horizontal motion.

To highlight the low frequency characteristic of the Emilia earthquake ground motion, in Figure 11e and 11f the decay of observed acceleration spectral ordinates (at 5% damping) of the horizontal components at 2s and 4s has been compared to that predicted by ITA10. (the coefficients necessary to predict the acceleration spectral ordinate at 4 s are not included in the original work and have been specifically evaluated for the present study following the same methodology). For the majority of EC8 C sites, within 100 km from the source, the discrepancy between median predictions and observations increases at increasing period. At T = 2s, observations are within the median plus one standard deviation, while at 4s the predictions strongly underestimate the observations, which are well above the mean plus one standard deviation. At distance larger than 100 km, the spectral ordinates, recorded mainly at rock/stiff sites, sharply decrease.

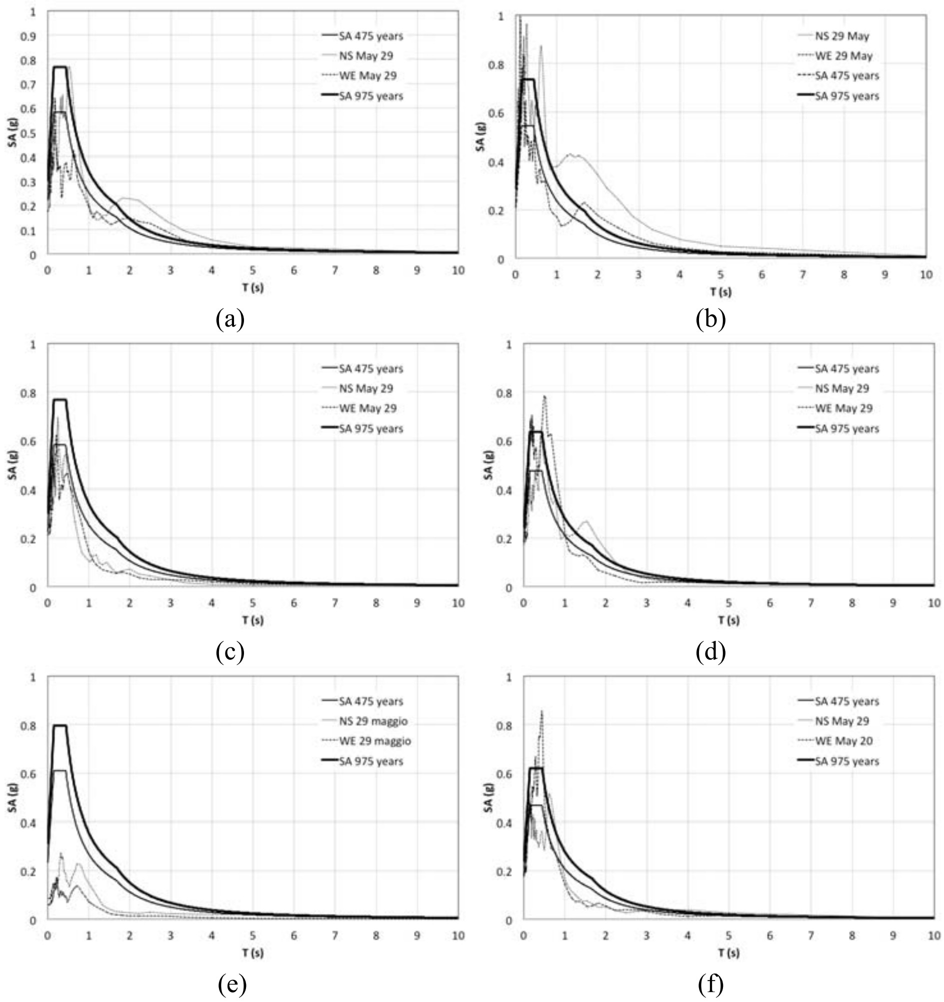

Fig. 10. a) MRN 3.5 km; b) SAN0, 4.7 km; c) FIN0 16.0 km; d) MOG0, 16.4 km e) RAV0, 15.6 km; f) SMS0, 14.9 km

a) b)

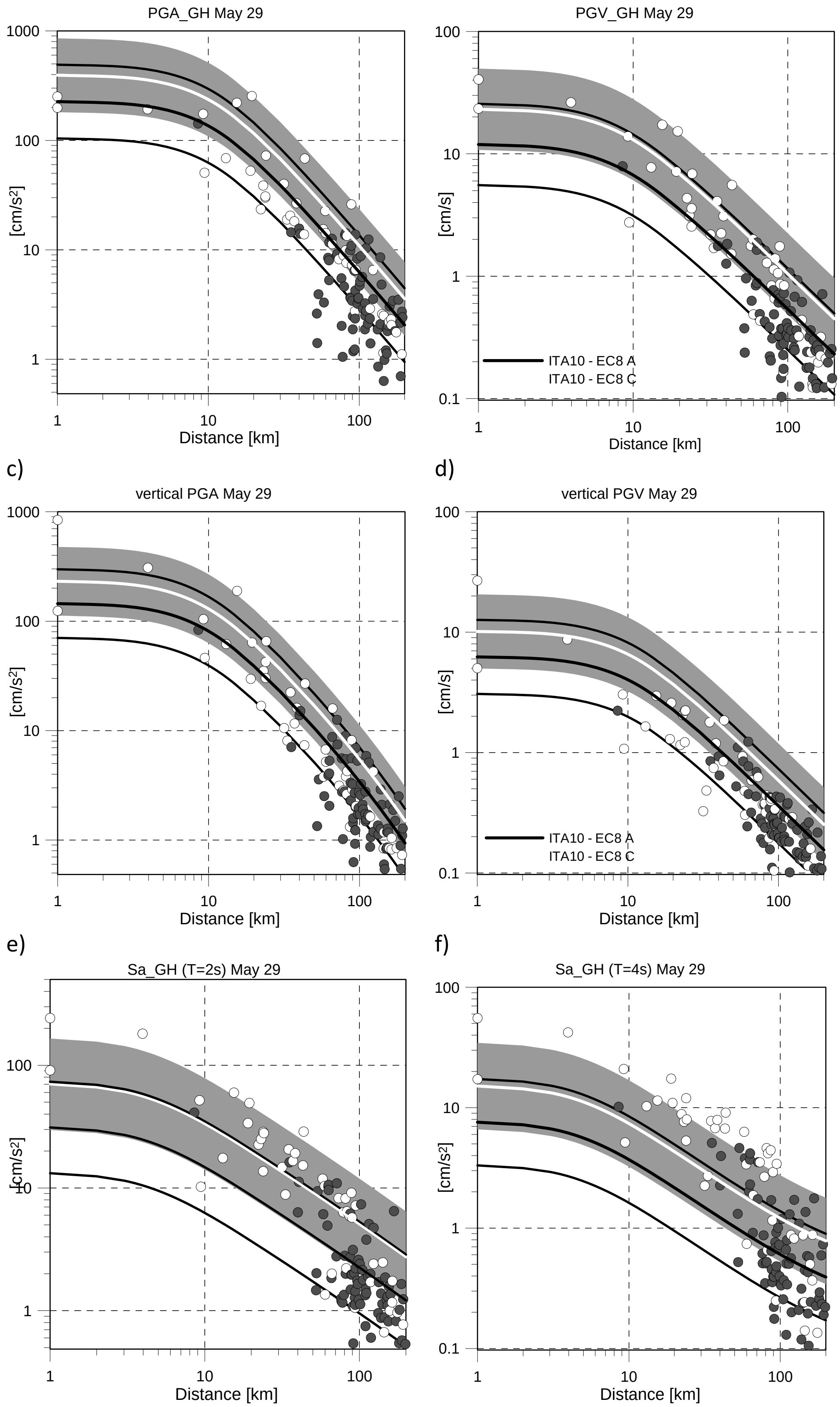

Fig.11. Comparison between observations and the prediction of a GMPE developed for Italy (Bindi et al., 2011)

Geomorphologic and hydrogeologic features

The Po Plain is bounded by the Alps and the Apennines and is the largest plain in Italy with a population of about 20 million people and a mean density of 450 inhabitants/km^2. Therefore, it is an area of high vulnerability in the occurrence of natural disasters. The hydrogeologic situation of the Po Plain is the result of the deposition vicissitudes of the water courses that have flowed through it since the filling up of the Pliocene sea by Quaternary alluvial sediments (since 0.4 Ma BP).
The area affected by the seismic sequence of 2012 corresponds to the southern sector of the central Po Plain (Fig.12).

Geomorphologic research carried out in the past decades has produced several maps and papers from which the Geomorphologic Map of the Po Plain at the 1:250,000 scale (Castiglioni *et al.,* 1997) and its illustrative notes (Castiglioni and Pellegrini, 2001) were derived.

Apart from the Po River – the largest river in Italy – the main rivers in the study area are the Secchia, Panaro and Reno which flow northwards from the Apennine foot.

The surficial alluvial deposits are Holocene in age. Their particle-size distribution is mainly silt and clay with sand levels in correspondence with ancient riverbeds and crevasse splays. Their thickness is variable from hundreds of meters to thousands of meters, depending on the local depth of the Apennine buried structures, known in literature as "Ferrara Folds" (Pieri and Groppi, 1981). These deposits are due to fluvial aggradation of both the Po and its Apennine tributaries.

The ancient drainage system shows clear evidence of two preferential directions. Proceeding towards the Po River from the Apennine foot, it changes sharply from a SSW-NNE direction to a W-E direction, starting in correspondence with the Carpi – Cento – S. Agostino alignment (Fig.12). The Apennine ancient riverbeds (Secchia, Panaro and Reno) seem to have been particularly affected by this shift of nearly 90°, whereas the old courses of the Po River maintained a W-E orientation. The ancient drainage network also shows that in their distal path, the Apennine ancient riverbeds were set in a direction parallel to the Po River before converging into it. This characteristic was lost only after human activities carried out on the drainage system in the past four centuries.

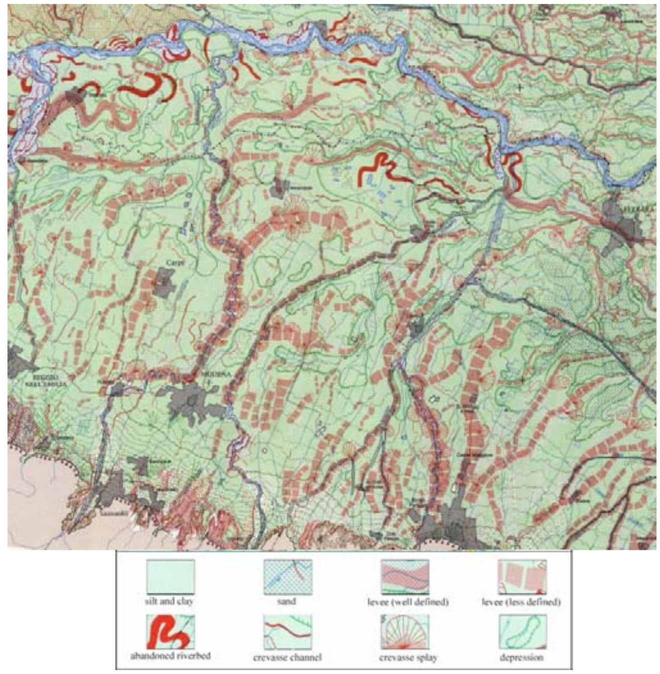

Fig. 12. Geomorphologic Map of the Po Plain epicentral area at the 1:250,000 scale (Castiglioni et al., 1997).

At the Apennine foot, the watercourses flowing into the plain built up north-stretching alluvial fans. Many levee ridges depart from the front of the fans and continue as far as the Po R (Figs.12 and 13).; their patterns reveal recent changes of path (Castiglioni et al., 1997; Castiglioni and Pellegrini, 2001). The levee ridges, that are located NE of Finale Emilia and S. Agostino, are particularly evident, even in the field. The levee ridge (Finale Emilia) belongs to an old Panaro riverbed active until the end of the 19th century whereas the latter (Sant'Agostino) belongs to an old Reno riverbed active until the mid-18th century. Less evident sandy ridges, corresponding to Panaro and Reno ancient riverbeds, are located between Cento and Finale Emilia. In the Mirandola area some levee ridges with a WSW-ENE trend, belonging to the Secchia R. ancient riverbeds, may be found.

North of Modena, lowland areas are found in-between fluvial ridges. In the area East of Mirandola an old meandering river path is well depicted in aerial photographs which clearly show two fluvial bends. This ancient riverbed is located between the Po, Panaro and Secchia rivers in an altimetric depression which was inundated many times by the Po R. As a consequence, flood clay sediments buried the older hydrographic features and sand sediments. According to detailed morphometric and geochemical analyses, this ancient riverbed (active in the Bronze Age) has been ascribed to the Po River (Castaldini *et al*., 1992).

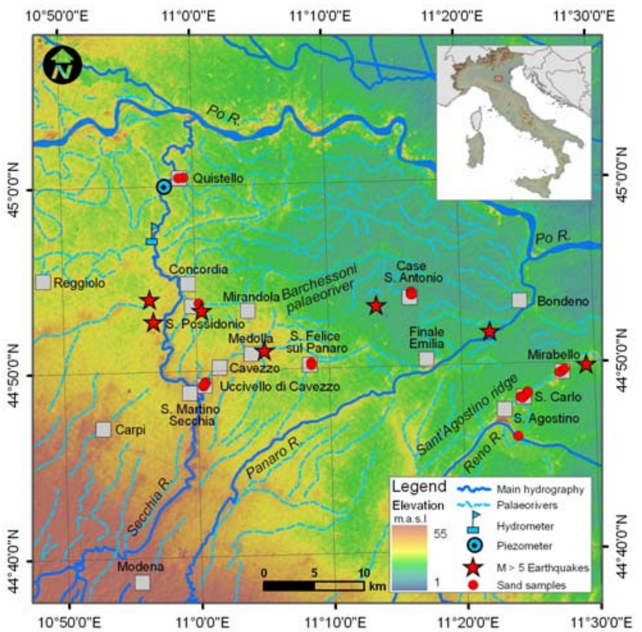

Fig.13. SRTM (Shuttle Radar Topography Mission; ~90 m cell size), red dots represent the location of liquefaction related phenomena. Sand samples have been collected at these sites. Most of the "liquefaction" sites are located on elevated fluvial ridges.

Taking into account the present-day hydrographic pattern, rivers flow deep in the upper part of the alluvial plain whereas in the mid-lower part of the plain the riverbeds are high over the surrounding territory and are confined within man-made dykes.

The geomorphologic framework of the study area is therefore characterized by complex drainage and ancient drainage patterns of the Po, Secchia, Panaro and Reno rivers, strongly influenced by the climate, tectonic and human activities.

As regards the present hydrogeologic situation, the grain-size distribution is extremely variable from place to place, due to frequent changes of path that affected the rivers and creeks in the past and, as a consequence, also the hydraulic conductivity is extremely variable.

The subsoil of the territory stretching from Cavezzo to S. Agostino is prevalently made up of aquitard or aquiclude silty-clayey sequences with levels of sand corresponding to ancient riverbeds or flooding events. Generally speaking, this area is therefore poor in groundwater resources apart from the sand fluvial deposits which, owing to their high hydraulic conductivity, make up small, confined aquifers scattered all over the low plain (Pellegrini and Zavatti, 1980). These lithological bodies, which are fed directly by precipitation or slow percolation from the surrounding thinner sediments, are often in a saturated state. North of the Mirandola-Finale Emilia alignment, the surface soil is still predominantly silty-clay, although at a depth of some 12 m the coarser, sandy deposits, corresponding to ancient riverbeds of the Po River, are found which contain pressurized groundwater mostly recharged by the river itself (Di Dio, 1998).

Notwithstanding the amount of water stored in these shallow aquifers, its chemical characteristics are poor since it comes in direct contact with the deeper, salty groundwater contained within the marine formations (Gorgoni *et al.,* 1982). The latter, owing to the structural characteristics of the bedrock (the subsurface folded and thrust anticline ridges known as "Ferrara Folds" – Pieri and Groppi 1981) is pushed upwards nearly as far as the ground surface.

From the standpoint of water resources, the whole area is therefore characterized by low-quality groundwater, so much so that local aqueducts extract and convey water directly from the upper plain area, where the hydrologic situation is much more favorable. The widespread presence of saturated sand deposits all over the lower plain south of the Po River make them prone to undergo soil liquefaction when subject to strong seismic shocks (Mw > 5.5), as occurred in the study area.

<u>Historical liquefaction of the interested area</u>

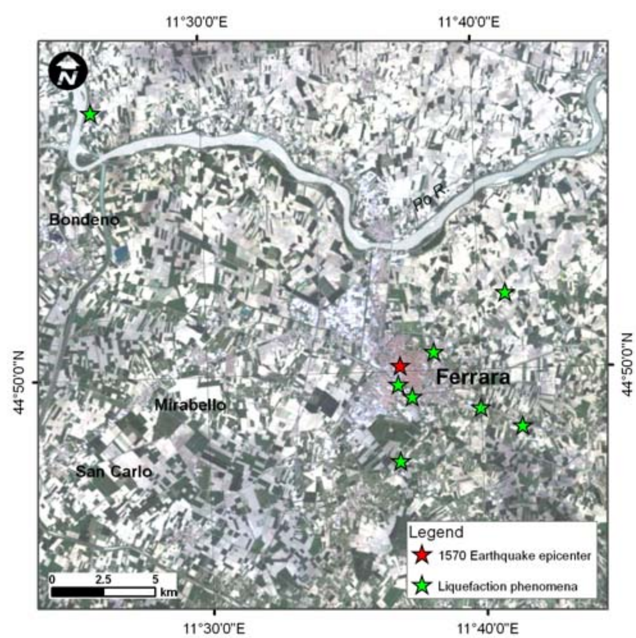

Fig.14. Liquefaction phenomena induced by the 1570 earthquake.

Several empirical databases (Kuribayashi and Tatsuoka 1975, Liu and Xie 1984, Ambraseys 1988, Wakamatsu 1991, 1993), correlating the occurrence of liquefaction with epicentral distance and magnitude, show that earthquakes of 4.2 and 4.8 magnitude can produce liquefaction-related phenomena in the proximity of the epicentral area (this is confirmed by the database of historical liquefaction in Italy – Galli, 2000;

Prestininzi and Romeo, 2000). The May 20th M5.9 and May 29th M5.8 shocks are examples of moderate earthquakes inducing such a phenomena. The previously mentioned database also indicates that an M5.9 earthquake can induce liquefaction phenomena at distances in between 10 – 40 km from its epicenter.

According to historical sources, the studied area has not been affected by events with epicentral intensity Io>6 MCS (Galli *et al.* 2012). The first strong earthquake seems to have occurred in February 1346, but little information is available (Galli *et al.* 2012). The historical seismicity of the area (Locati *et al.* 2011) shows the occurrence of two moderate events since the 16th century (1570 Ferrara and 1624 Argenta earthquakes, Guidoboni *et al*. 2007). During both events, liquefaction occurred in adjacent urbanized areas. The strongest event took place on November 17, 1570 (Io 7-8 MCS, Mw 5.46) about 35 km from the 2012 epicenters (Fig.14). The 1570 sequence recorded more mainshocks and many localities were affected by liquefaction (Galli, 2000), which occurred mainly around Ferrara and up to Ficarolo, on the left bank of the Po River.

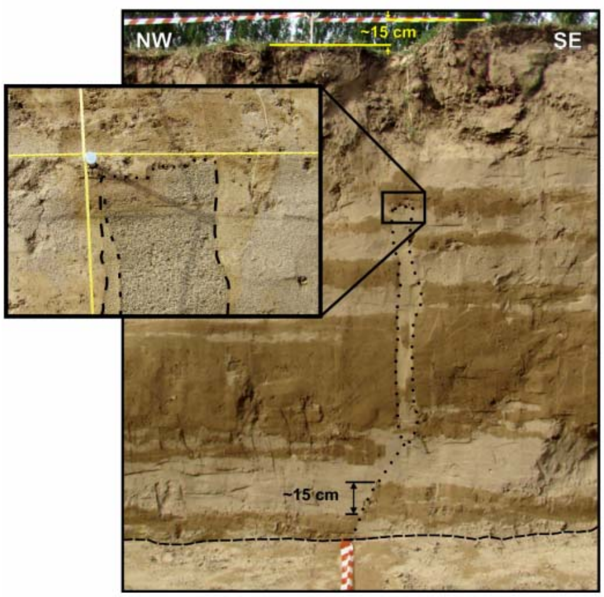

Fig.15. Example of a thick sand-filled dike clearly sealed by younger sedimentary beds, thus emphasizing the occurrence of liquefaction events older than the May 2012 earthquake (Caputo et al., 2012)

Recent studies have retrieved the traces of other damaging earthquakes occurring between the 1600s and the 1700s and had been overlooked by the seismological literature (Castelli *et. al*., 2012). Two minor quakes are reported by DBMI11 (the Italian macroseismic database; Locati *et al*., 2011) within the 2012 mesoseismic area: one occurred on December 6, 1986 (Mw=4.35), on July 11, 1987 a Mw = 4.56 event struck the Po Plain between Bologna and Ferrara.

Further documentation of the occurrence of liquefaction events older than the May 2012 earthquakes is provided by palaeo-sismologic studies carried out after the May 2012 bearthquakes in some trenches excavated south of the village of San Carlo (Caputo *et al.*, 2012). Figure 15 shows a picture of the trench with structural evidences of ancient liquefaction. Caputo *et al.* (2012) suggest that the earthquakes of 1570 and 1624 could be the events that have induced these old liquefaction phenomena.

Soil liquefaction induced by the May 20th and May 29th earthquakes and geomorphologic characterization of the liquefied areas

The May 20, 2012 M5.9 and May 29, 2012 M5.8 events are examples of moderate earthquakes yielding extensive liquefaction, which occurred over an area with a 21.5 km radius from the epicenter of the May 20 quake (Pizzi and Scisciani, 2012) and induced several damages of buildings and infrastructures. Some 700 liquefaction cases were recorded (see Bertolini and Fioroni, 2012; Crespellani et al., 2012; Di Manna et al., 2012; Pizzi and Scisciani, 2012; Vannucchi et al., 2012). These phenomena concentrate along alignments which follow the abandoned riverbeds (Secchia, Reno, Panaro and Po rivers) (Fig.16). Soil liquefaction and ground cracks were accompanied by sand boils. Photogrammetric surveys were carried out on several sand boils belonging to some representative liquefaction features using digital reflex cameras with calibrated 20 mm fixed lens (Ninfo *et al.*, 2012). In order to study the micro-morphology of the sand boils DEMs with resolutions ranging from 1 millimeter for the smaller forms to some centimeters for the large ones were built.

Fig. 16. Alignment of sand boils in correspondence with a Po ancient riverbed (Case San Antonio, Bondeno Municipality).

Fig. 17. Ejected sand in the San Agostino cemetery.

The zone with the most evident and widespread effects induced by the first main shocks (May 20) is that around S. Carlo belonging to S. Agostino municipality. S. Carlo, as well as the nearby village of Mirabello, is located about 17 km east of the epicenter on a fluvial ridge corresponding to a Reno R. ancient channel known as "S.'Agostino ridge" (Castaldini and Raimondi, 1985). The ancient riverbed of the Reno River was active between medieval times and the end of the 18th century when it was subject to an artificial diversion near S. Agostino village (Castaldini and Raimondi 1985, Castaldini 1989b) in order to eliminate the recurrent floods that affected the surrounding plain. It has a SW-NE trend and is a very evident morphologic feature, 3 to 4 m higher than the surrounding territory. Liquefaction was detected along the SW-NE alignment of the old Reno River alluvial plain. Numerous buildings lie on this sandy ridge. At this site a large quantity of sand was ejected from the subsoil and caused major damages to the village of S. Carlo (Fig.17-18).

Fig. 18. Settlement of shallow foundation of a cottage because of liquefaction (S. Carlo).

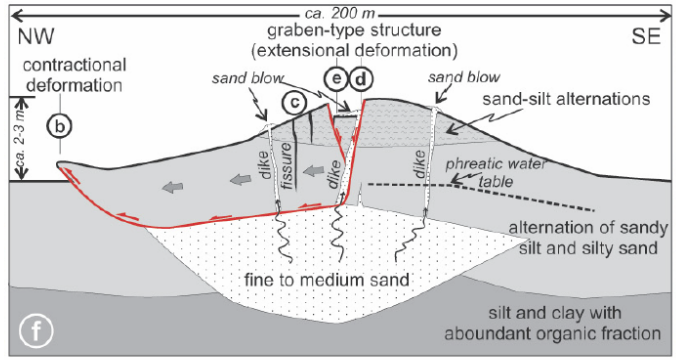

Fig. 19 – Possible interpretation (lateral spreading along the NW slope of an ancient riverbed) of soil liquefaction observed at the Sant'Agostino cemetery (Pizzi and Scisciani, 2012)

The abandoned bed of the Reno River, is mostly characterized by sand, interbedded by finer layers of clay and silt. In S. Carlo detailed geologic, geotechnical and geophysical surveys were carried out in order to reconstruct the geological model of the subsoil (15 to 20 m in depth) (Gruppo di lavoro, 2012, Lai *et al*, 2012). According to these investigations, the embankment consists of an alternation of sand and silt for a total thickness of about 4 m. Alternation of sandy silt and silty sand extend for another 6 m from ground level. Locally a 4 m thick lens of fine and medium sand, corresponding to the ancient Reno riverbed, is present. Clay and silt deposits with an abundant organic fraction and a constant thickness of 9 to 10 m were then found overlying alternation of sandy silt and silty sand (Fig.19).

Borehole logs (carried out before the seismic sequence) at S. Carlo show that water table is about 3 m below the ground level. Analysis of borehole logs and geologic surveys revealed high spatial variability of soil characteristics, especially in the upper layers. The lateral heterogeneity of soil formations is confirmed by the results of CPT tests and is consistent with the observations made during surveys on whether or not liquefaction has occurred at closely-spaced sites.

Lateral heterogeneity in San Carlo is also a consequence of the construction of river dykes for flood prevention and of artificial sand fills.

The horizon affected by liquefaction is a lens of fine and medium sand located at 4 m (plain zone) and at 6 m (ancient bankfill) respectively below the ground level.

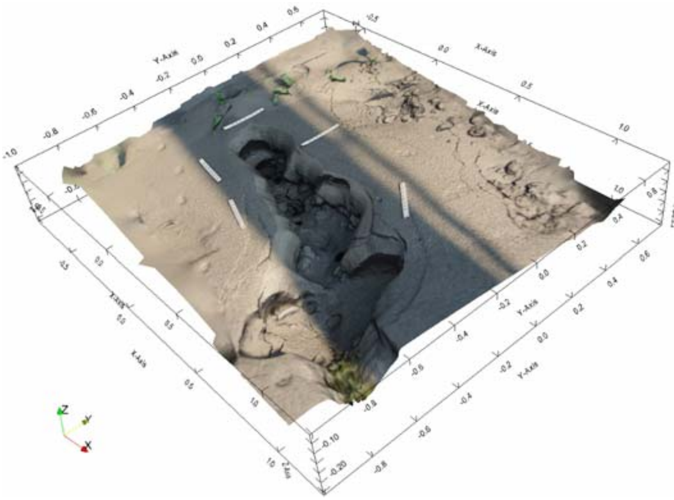

Fig. 20. 3D reconstruction of a fracture associated with sand boils in corn field near Case S. Antonio.

Other significant liquefaction effects caused by the May 20 earthquake were observed at Case S. Antonio (Bondeno Municipality) (Fig.20) at the boundary with Finale Emilia Municipality, which was the epicenter of the May 20, 2012 earthquake (M = 5.9). By the middle of July, the coseismic effects (sand boils) were no longer visible in the field as they were hidden by the crops (mainly corn) and were later obliterated by farming practices and precipitation. From a geomorphologic viewpoint the site is located between the Po, Panaro and Secchia rivers, in the lowest sector of the Modena plain (8 - 9 m a.s.l.). This area was flooded many times by the Po River and the clayey sediments buried older fluvial sandy deposits and archaeological settlements. The liquefied material belongs to the sediments of a ancient riverbed known in literature as "Barchessoni ancient riverbed". The geochemical analysis of sediments and the meander geometry of the "Barchessoni ancient riverbed" have shown more similarity with the present day Po River than the Secchia and Panaro rivers (Castaldini et al. 1992). Archaeological settlements found here have revealed that this Po ancient riverbed was active in the Bronze Age (Balista et al. 2003). In the Iron Age and in the Roman times it was a small watercourse; the period in which the complete extinction of the channel took place, remains unknown (Castaldini et al. 2009).

The S. Felice sul Panaro liquefaction features were produced by the May 20th earthquake and were reactivated by the May 29th shock. S. Felice sul Panaro (17 m a.s.l.) is located in a sector where silt and clay deposits crop out (Castaldini *et al.* 1989b, Castiglioni *et al.* 1997). Important liquefaction effects occurred in the urban area (in the stadium and in a school yard) that lies at the confluence of a S-N Panaro ancient channel and a W-E flowing ancient riverbed of the Secchia R.. These were active in Roman and Medieval times (Castaldini et al. 1989b). Nowadays the sand sediments have been removed by human activities.

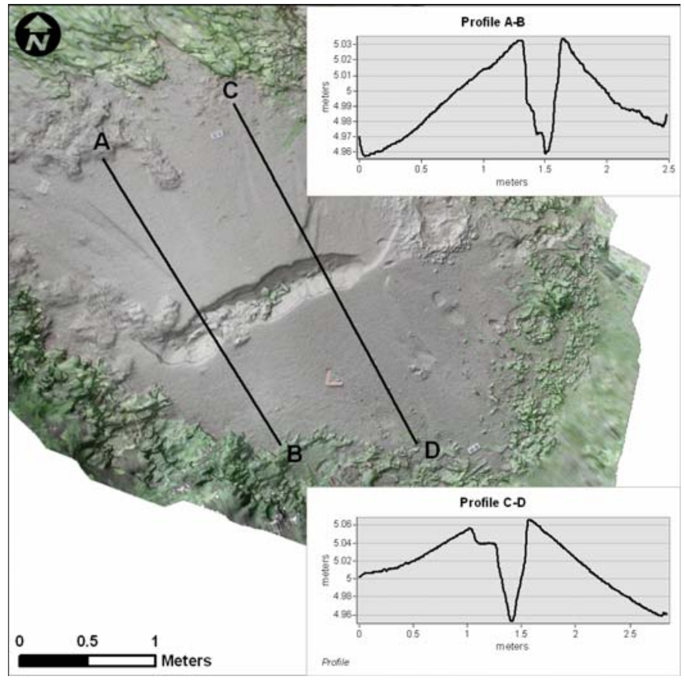

Fig. 21. Isolated sand boil oriented N64° near Uccivello di Cavezzo

Liquefaction phenomena at Uccivello di Cavezzo (Fig.21), S. Possidonio and Quistello were triggered by the May 29th (M= 5.8) earthquake. Uccivello di Cavezzo and S. Possidonio are located on an ancient course of the Secchia River (Castaldini 1989a, 1989b). Uccivello di Cavezzo (23 m a.s.l.) is on the Secchia fluvial ridge, which is NW-SE orientated and crosses S. Martino Secchia, Cavezzo and Medolla. It was active during Roman and Medieval times until the 13th century. Just one week after the earthquake, the sand boils in the fields were removed by agricultural works. Also S.Possidonio (20 m a.s.l.) lies on a NW-SE trending sandy fluvial ridge corresponding to a Secchia ancient riverbed, which was abandoned in modern times. In all liquefaction events the areal extension of ejected material range from a few square meters up to many hundreds square meters. The cone height is generally lower than 30-40 cm, the cones are in most cases aligned. The most visible alignments of liquefaction, surface fracturing and sand ejection are represented by the liquefaction phenomena observed from S. Agostino to the Mirabello municipalities (SW-NE following the old Reno river plain) and of Cavezzo (NE-SW following the ancient channel of the Secchia River), which are several kilometers long.

Fig. 22. Ground ruptures in S. Carlo.

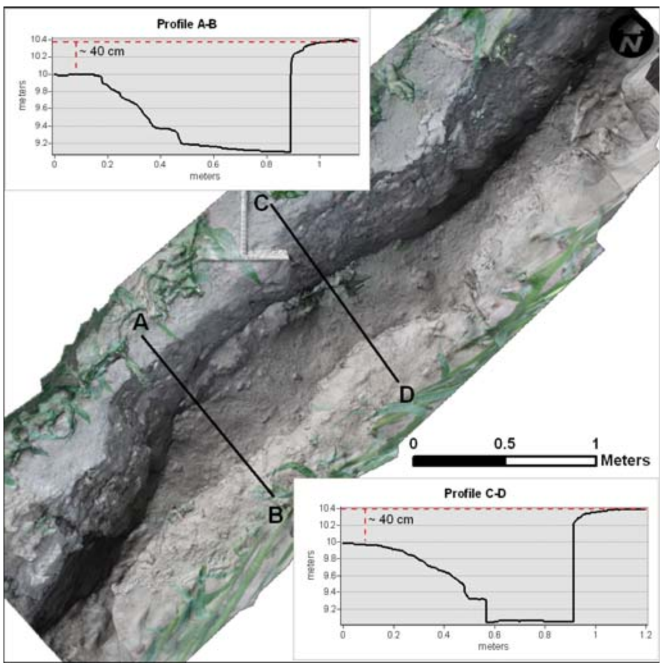

Fig. 23. Fracture in a corn field located immediately west of the village of S. Carlo. It has an average width exceeding 50 cm and a depth that locally exceeds 1e meter. It is characterized by a N 44° direction and by a vertical displacement of the NW block of about 40 cm. This ground cracks is continuous from S. Carlo to S. Agostino.

Ground cracks were also widespread and affected paved roads, buildings and farmed land. The ground ruptures damaged all the constructions above them, especially the houses in S. Carlo and the industrial settlements between S. Carlo and Mirabello. In the residential area located close to a corn field affected by these cracks (Fig.22-23) there is another N60° oriented ground crack system (Fig.24). This system affects De Gasperi and Morandi streets causing several failures of the road surfaces and breaking underground infrastructures like gas and water pipes.

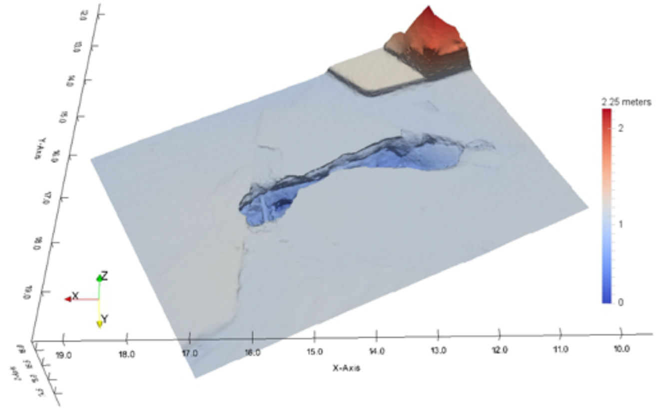

Fig. 24. N59° oriented fracture located in Morandi street in S. Carlo.

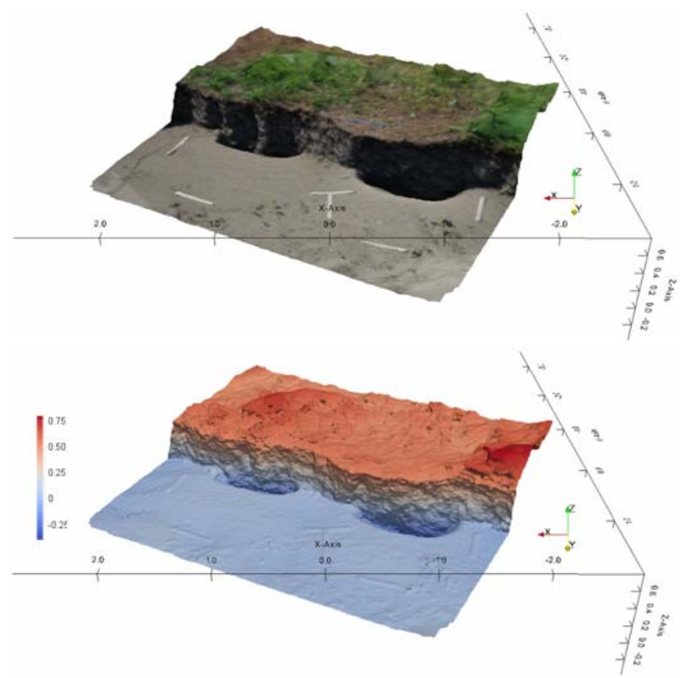

Fig. 25. A fracture located in Via Rossini and connected with the previously described fracture system located in the village of S. Carlo. Vertical displacement here is about 15 to 20 cm.

The main fracture system crosses all the village of San Carlo following the Reno ancient riverbed. In the North-eastern part (Rossini street) the fractures are often characterized by vertical displacement of ~20 – 40 cm and by the presence of sand boils (Fig.25).

Proceeding to the south west towards the Sant'Agostino cemetery, the intersection of two ground cracks oriented N39° and N50° generates a small horst - graben structure (Fig.26).

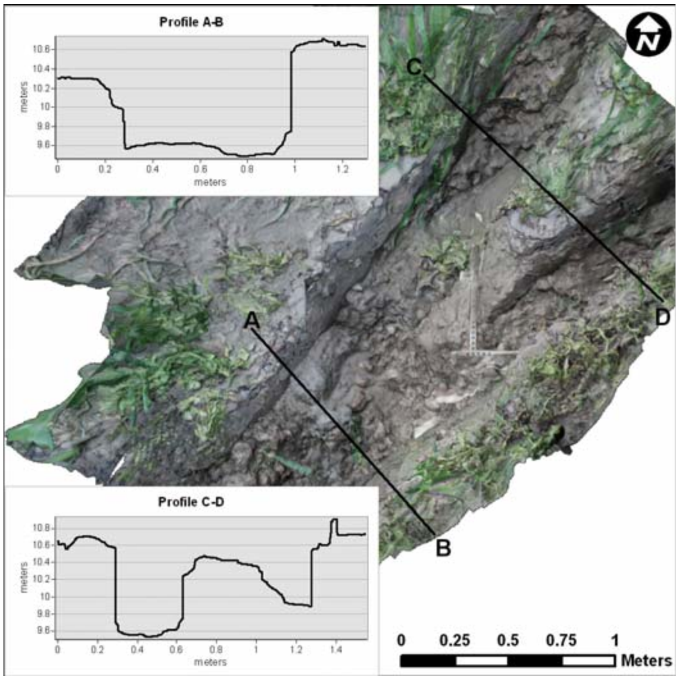

Fig. 26. Horst-graben structure. Even in this case the maximum depth reaches 1 m whereas vertical displacement is around 30 cm.

Fig. 27 – Uccivello di Cavezzo: bed of a canal uplifted, bulged and cracked due to sand ejection from beneath its bottom after the 29th May earthquake.

After the 20th May earthquake some buildings of S. Carlo were declared totally or partially unsafe, some roads were closed and some lifelines were destroyed (Mirabello). The May 29th shocks did not worsen the damage. In S. Carlo the most damaged houses are located on top of the Reno ancient riverbed embankment pointing out that the topographic effect (lateral spread) played an important role.

Ground ruptures are also evident at the Mirabello stadium on the embankment of ancient riverbed of Reno River. The lateral spreading occurring along the levees of this ancient channel, from S. Agostino to Mirabello were responsible for ground ruptures (Fig. 19).

In some places also the bottom of canals and ditches showed uplift, bulging and cracks due to sand ejection from beneath the bottom of these minor watercourses channel (Fig.27-28-29).

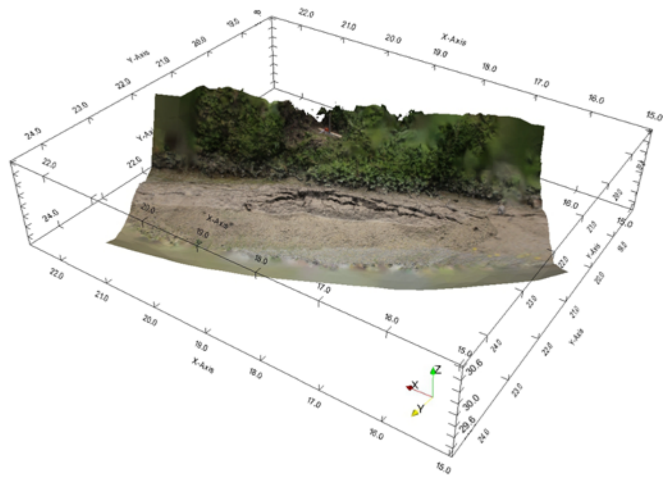

Fig. 28. 3D representation of sand ejection from beneath the bottom of a canal at Uccivello di Cavezzo after the May 29th earthquake.

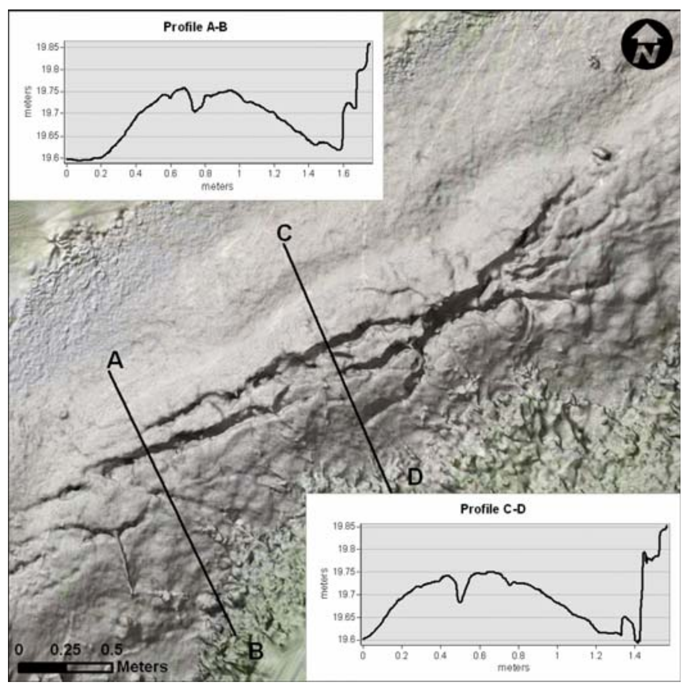

Fig. 29. Profile of the channel bed: vertical uplift is ~15 cm.

Another effect of the earthquakes was the ejection of sand from water wells (Fig.30).

Hydrogeological anomalies were also recorded. Some automatic stations of the Emilia-Romagna (Arpa Emilia Romagna 2012) regional well network recorded water level variations (Marcaccio and Martinelli, 2012) with uprising phenomena up to 1.5 meter.

Fig. 30. Ejection of sand from water well (S. Carlo).

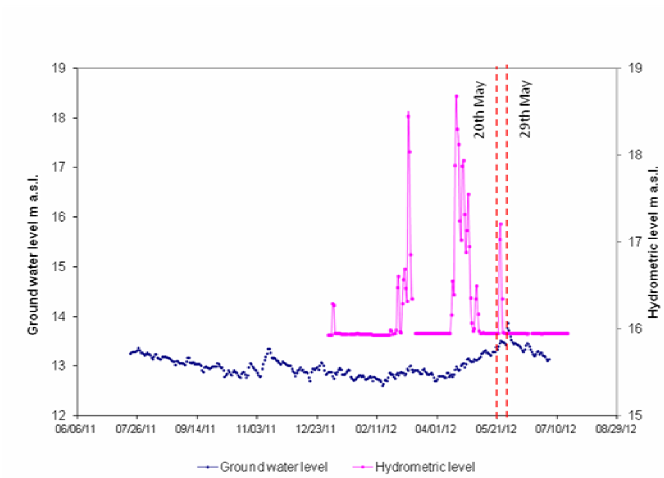

Fig. 31. Variations of groundwater level in a piezometer located at Quistello (24 km from the May 20th earthquake and 19 km from the May 29th quake epicenters) and water level variations of the Secchia River at Bondanello (Arpa Emilia-Romagna, 2012) 23 km from the May 20th quake and 16 km from the May 29th quake).

It is also very interesting to show the variations with time of piezometric elevation in a monitored piezometer at Quistello and of the water level of the Secchia River at Bondanello (Fig. 31 and Fig.32). The distance between the piezometer at Quistello and the hydrometer at Bondanello is about 5 km. More specifically, Figure 32 shows the piezometric elevation at Quistello (also shown in Figure 31) using an enlarged scale.

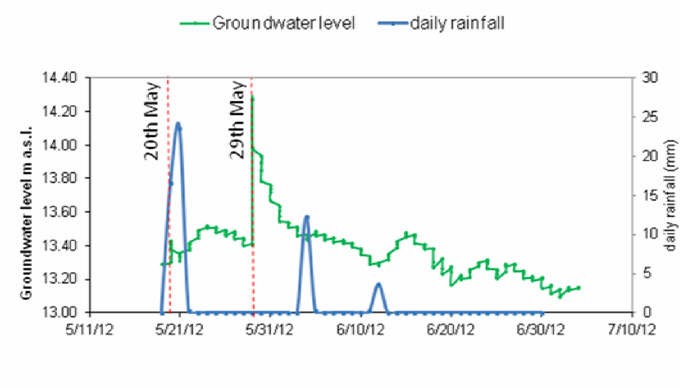

Fig. 32. Groundwater level variations in the May 19th – July 2nd 2012 period in the Quistello piezometer. Reading delay of piezometer: 3 hours with respect to the May 20th shock; 4 hours with respect to the May 29th shock.

The Figures also indicate the epicentral distance for the considered event and the reading delay with respect to the occurrence of the event considered. Figure 33 shows the piezometer scheme (Quistello), the soil stratigraphy as inferred from geotechnical borehole and the cone resistance & friction ratio (qc – Rf) profiles as inferred from mechanical CPTs (both borehole and CPT were carried out before the seismic sequence). The piezometer is located on the right side of the Secchia River embankment. It should pointed out that at Quistello the first 3 m consist of fine silty sands (Dr=70-100%, γ=18.5 kN/m^3, qc=3-10 MPa) overtopping a 3 m thick layer of silty clay (cu=44-73 kPa; γ = 19 kN/m^3; qc=3.7-5.5 MPa). After the clay layer the soil deposit consists of sand and silty sand up to a depth of 40 m (Dr=55-75%; qc=8.8-23.5 MPa). At the testing time (September 2003), the water table was at 4.3 m deep from the ground level.

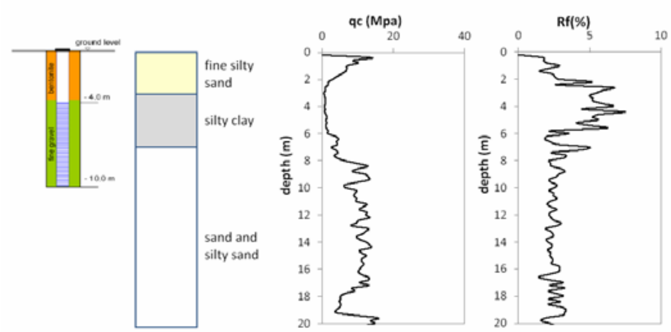

Fig. 33. Piezometer schemes, the soil stratigraphy and CPT penetrometric test at Quistello.

Piezometric elevation (at Quistello) was recorded every 6 hours in an open pipe piezometer (depth = 10 m) where a HOBO U20 Water Level Data Logger was installed.

Information about rainfall were also considered, referring to the Palidano di Gonzaga rain gauge (located 16 km from the Quistello piezometer and 15.km from the Bondanello hydrometer). Figure 31 shows the ground water level fluctuations from July 2011 to July 2012 (Quistello piezometer). The water level changes of the Secchia River at Bondanello are also reported for the Jannuary 2012-July 2012 period. The Secchia River level is located at a lower elevation in relation to the hydrometric level (15.95 meters). The peaks in the graph are related to short floods of about 1.5 m, that were not able to influence the shallow water table. During the May 29th earthquake a little flood occurred, causing an uplift of the Secchia River of about 1.25 m. Nevertheless, the flood run out in 48 hours and the river level came again to the hydrometric zero. In addition, after the May 29th earthquake the piezometric pressure showed an increase of 8 kPa, equal to a short-lasting uplift of 86 cm (Fig. 32) of the shallow water table followed by a more longer return (14 days). The anomaly fit with the date of earthquake and no rainfall was recorded in the same period. It can therefore be stated that the anomaly was seismically induced. The May 29th seismic event occurred at a distance of about 19 km from the monitoring station.

The May 20th earthquake did not induce so visible groundwater level changes, which were less than 12 cm (Fig.32). The first measurement of the piezometric elevation after the M = 5.9 shock (May20th) was recorded about 4 hours after the seismic event.

<u>Geotechnical characterization of the liquefied areas and preliminary check of the liquefaction susceptibility</u>

The geotechnical characterization of the liquefied sites is based on the following information:

- 23 grain-size distribution curves of the ejected soil; the samples have been retrieved from the sites located in Figure 13;
- 4 additional grain size distribution curves of the ejected soil at S. Carlo (mentioned by Lai *et al.* 2012);
- 5 boreholes carried out in the 1980s at S. Carlo with SPT measurements (mentioned by Lai *et al.* 2012);
- 9 mechanical CPT carried out at Mirabello (about 6 km far away from S. Carlo) on 1985. The penetration depth is 8 m;
- 13 mechanical CPTs carried out at S. Carlo on 1985. The penetration depth is generally 8 m to 10 m;
- 11 mechanical CPTs carried out at S. Agostino on 1992 and 1995 with a penetration depth of 10 m to 30 m;
- one borehole carried out at S. Agostino in 1975 up to a depth of 40 m with several SPT measurements;
- MASW, ReMi (Achenbach 1999, Aki and Richards 1980), and Nakamura H/V (Nakamura and Ueno 1986) tests were carried out in San Carlo on May 29th 2012 (after the second main shock) at four different sites that exhibited liquefaction phenomena (Lai *et al.*, 2012).

Locations of CPTs in Mirabello,, S. Carlo and S. Agostino considered in this report are shown in Figure 32.

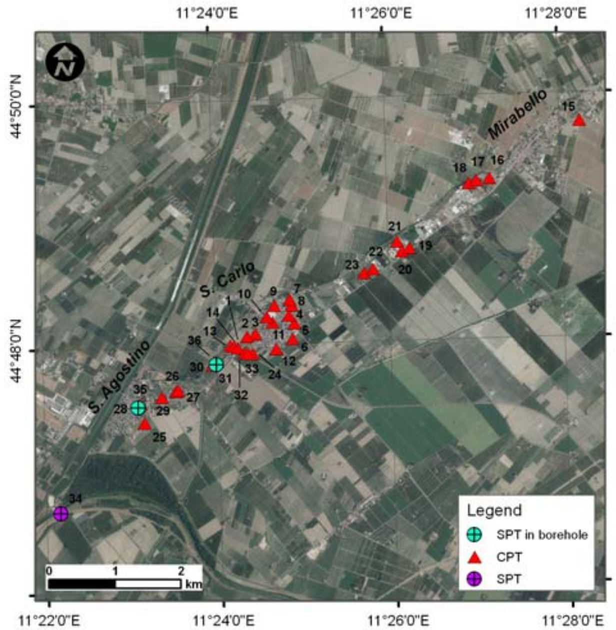

Fig.34 Location of CPTs in Mirabello, S. Carlo and S. Agostino.

Figure 35 and Table 2 respectively show the grain size distribution curves of the soil retrieved from the sites where liquefaction was observed (Figure 13, Gruppo di Lavoro 2012) and grain-size characteristics of the same samples. The figure also shows the grain size interval (for well graded materials) of liquefiable soils according to NTC (2008). The limit curves, proposed by Obermaier (1996) for defining the grain size distribution of liquefiable soils, are also shown.

Most of the tested samples are uniform. On the whole, the uniformity coefficient (U_c) is in between 2 and 9 with a fine fraction ranging from 4 to 60%. The samples with the highest uniformity coefficient are from Uccivello di Cavezzo (Uc>5), S. Felice sul Panaro and S. Carlo where the amount of fines content (FC = materials passing a number 200 sieve ASTM) is generally up to 12%. These are classified as silty sand or sandy silt. In the area of Case S. Antonio and Quistello the collected samples are uniform and their grain size ranges from sand (FC < 5%) to silty sand (FC > 12%).
The same indications are obtained from the data shown by Lai *et al.* (2012).

Preliminary assessment of liquefaction susceptibility has been done following the current practice (Kramer 1996) and the Italian Building Code (NTC 2008). More specifically four different aspects have been considered.

As for the driving forces:
It is self – evident that the two main shocks were capable of inducing liquefaction phenomena. The Italian Building Code (for e return period of 475 years) considers a Magnitude greater than or equal to 5 and a PGA > 0.1 g.

As for the geological aspects:
The paragraph on hydrogeology and geomorphology has clearly pointed out that the liquefaction phenomena occurred along palaeo – riverbeds. The existence of a large area prone to the occurrence of liquefaction has also been demonstrated.

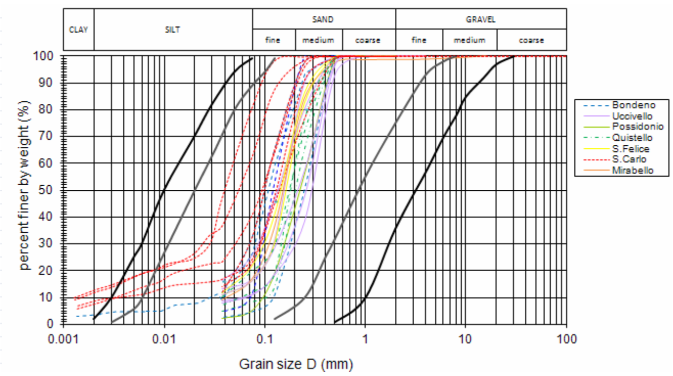

Fig. 35. Grain size distribution of liquefied soils. The black lines correspond to the boundaries for potentially liquefiable soils (Obermeier 1996); the grey lines represent the interval with high potentially liquefiable soils (uniformity coefficient > 3.5).

Table 2. Grain-size characteristics of the liquefied soils. FC = materials passing a number 200 sieve ASTM, D_{50} = mean grain size, U_c = coefficient of uniformity

Site	**Fluvial domain**	**D50 (mm)**	**FC (%)**	**sand (%)**
Case. S. Antonio	Po ancient riverbed	0.1-0.25	5-32	68-88
Uccivello di Cavezzo	Secchia ancient riverbed	0.15-0.3	11-25	68-88
S. Possidonio	Secchia ancient riverbed	0.22	4	96
Quistello	Po ancient riverbed	0.18-0.2	8-19	81-92
S. Felice sul Panaro	Panaro ancient riverbed	0.15-0.18	22	78
Mirabello	Reno ancient riverbed	0.18	16	84
S. Carlo	Reno ancient riverbed (fractures)	0.04-0.09	41-80	59-20
S. Carlo	Reno ancient riverbed (sand boils)	0.12-0.15	17-24	76-83

Table 3. Identification of liquefiable layers (CPT results, Youd *et al*. method)

Location	Test Number	Label in Fig. 32	Depth (m)	Fs (-)	Soil type
Mirabello	185140C024	15	3.6 – 4.2	0.93 – 1.1	Sand to silty sand
Mirabello	185140C027	16	5.4 – 5.8	0.88 – 1.0	Sand
Mirabello	185140C028	17	4.2 – 4.4	1.0	Sand
Mirabello	185140C029	18	3.6 – 4.2	0.96 – 1.0	Silty sand
Mirabello	185140C030	19	-	-	Clay
Mirabello	185140C031	20	4.6 – 4.8	1.1	Sand
Mirabello	185140C032	21	-	-	Clay
Mirabello	185140C033	22	4.4 - 4.6 6.2 – 6.4 6.8 – 8.0	1.0 0.95 0.90 – 1.13	Silty sand Sand Sand
Mirabello	185140C034	23	0.4 – 0.6 2.0 – 2.2 5.2 – 5.4 5.8 – 6.0	0.95 1.1 0.8 1.0	Silty sand Silty sand Sand Sand
S. Carlo	185130C001	1	5.6 - 7.8	0.7 – 1.1	Sand
S. Carlo	185130C002	2	3.8 – 7.8	0.7 – 1.0	Sand
S. Carlo	185130C003	3	3.2 – 3.6 5.6 – 6.4	0.93 – 1.0 0.70 – 0.86	Sand Sand
S. Carlo	185130C004	4	3.6 – 6.6	0.77 – 1.0	Sand
S. Carlo	185130C005	5	4.4 – 6.8	0.86 – 1.0	Sand
S. Carlo	185130C006	6	4.2 – 5.0	0.78 – 1.1	Sand
S. Carlo	185130C007	7	4.6 – 5.4	0.89 – 1.0	Sand

S. Carlo	185130C008	8	-	-	Silty sand
S. Carlo	185130C009	9	-	-	Sand, Silty sand
S. Carlo	185130C010	10	-	-	Sand, Silty sand
S. Carlo	185130C011	11	-	-	Sand, Silty sand
S. Carlo	185130C015	12	1.2 – 4.2	0.8 – 1.0	Sand, Silty sand
S. Carlo	203010C041	24	4.6 – 6.2	0.66 – 0.96	Sand
S. Agostino	185130C050	13	-	-	Sand, Silty sand
S. Agostino	185130C051	14	8.6 – 11.0	0.84 -1.1	Sand
S. Agostino	203010C050	25	-	-	Clay
S. Agostino	203010C069	26	-	-	Sand, Silty sand
S. Agostino	203010C070	27	-	-	Sand, Silty sand
S. Agostino	203010C077	28	-	-	Sand, Silty sand
S. Agostino	203010C079D	29	9.2 – 11.2	1.0 – 1.1	Sand
S. Agostino	203010C083	30	-	-	Sand
S. Agostino	203010C084	31	-	-	Sand
S. Agostino	203010C0101	32	5.4 – 6.0	0.76 – 1.1	Sand
S. Agostino	203010C0102	33	5.4 – 6.0	0.83 – 1.0	Sand

As for the textural (compositional) aspects:
The particles size distribution curves of the investigated soils fall into the range of high possibility of liquefaction.
The compositional criteria confirm that the considered materials are susceptible to liquefaction. The compositional criteria prescribed by NTC (2008) and reported in Figure 35 exhibit a certain ambiguity as already observed by Lo Presti & Squeglia 2011. More specifically, it is not clear how to consider those curves having a tail exceeding the limits. In the present case all the samples have been retrieved from sand boils or other sediments of ejected soil.

As for the soil state aspects:
Lai *et al.* (2012) analyzed the available data in S. Carlo using both the deterministic approach (Youd *et al.* 2001) and the probabilistic approach (Idriss and Boulanger 2008). Two main conclusions were pointed out by Lai *et al.* (2012): the very high spatial variability of penetration resistance and the very low liquefaction potential. Only in one case they predicted a liquefaction induced settlement of about 13 cm. The SPT penetration resistances that led to such an evaluation have been obtained from one borehole exactly located where liquefaction phenomena had been observed.

The shear wave velocity profiles obtained by Lai *et al.* (2012) after the May 20th shock is in agreement with the above conclusions. Indeed, for the shallower layer (0 – 6 m) the measured shear wave velocity is generally 120 to 135 m/s and only for one of the four seismic lines a value of 105 m/s has been measured.

Table 3 summarizes the data of examined CPTs in Mirabello, S. Carlo and S. Agostino, indicating the values of the safety factor of less than 1.1, the depths where these low values have been observed and the main nature of the soil. Safety factor has been computed according to the method suggested by Youd *et al.* (2001).

Even though it is premature to draw definitive conclusions, it is possible to observe that simplified analyses based on CPT results indicate that the liquefiable soil is generally located at depth greater than 4 m and the thickness of the liquefiable soil is generally of few meters. Under these conditions, only minor effects of liquefaction are generally observed at the ground surface and the damages of buildings resting on shallow foundations are generally limited (ISSMGE 1999). What observed after the Emilia 2012 earthquakes seems to confirm this last statement.

It should also be pinpointed that liquefaction events were not randomly distributed, but appeared to be concentrated along the winding courses of abandoned rivers and their sandy deposits (cf. Bertolini and Fioroni, 2012; Di Manna et al., 2012). Therefore, also in alluvial plain areas seismic hazard assessment finalized to territorial planning should be based on a correct and thorough knowledge of the geomorphologic features and the surface and subsurface lithologic and hydrogeologic characteristics.

DAMAGES TO STRUCTURES

The earthquakes occurred in the Emilia region on May 20th and May 29th 2012 interested an area of about 900 km^2. A relevant set of public and private buildings, as well as industrial constructions, have been affected by different types of damages: particularly some collapses occurred in the industrial buildings represent a new aspect in seismic prevention and caused specific new regulations against that risk (www.protezionecivile.gov.it).
A large number of teams of engineers visited the entire area interested by the earthquakes to carry out safety inspections and the classification of damages and safety level. The group of the authors was involved in several inspection services in order to individuate the seismic damages of public and private buildings and to determine the level of safety by way of the AEDES form of the Civil Protection Service (Region of

Emilia Romagna) for schools, civic and social centres in the area of Reggiolo. Moreover, the authors took part to the group commissioned by Regional MiBAC Service (Ministry of Cultural Heritage) together with MiBAC architects, members of National Body of Fire Guards and structural engineers from Universities, to detect the damages of public buildings under historical regulation in the municipalities of Reggiolo, Carpi, Concordia sulla Secchia. The group established the level of damage surveying the main collapse mechanisms activated by the earthquakes. The buildings of Reggiolo subjected to inspection are summarized in table 4, with AEDES damage index (from A to E, where A=safe, B=safe after small works, C=partial unsafe, D= to verify again, E=completely iunsafe) and MiBAC damage index (0,00 = no damages; 1,00 = total collapse).

Report about Reggiolo.

Reggiolo is a city of about 9,200 inhabitants on a territory of about 43 km^2, with medieval origins and some important historical buildings (the Rock, the Town Hall, the Theatre, etc.) located in the city centre; a large series of masonry and r.c. constructions (mainly for housings) has been added in the urban expansions of the '900, together with several precasted r.c. constructions for public services (social centers, schools, sport activities etc.) and industrial plants. The city centre was built mainly by clay bricks with weak mortar: this is historically motivated by the lack of caves to produce lime for mortar in Emilia: probably also for that reason the main public constructions suffered severe damages, in most cases showing collapses along the mortar layers; the check of some collapsed walls highlighted an insufficient adhesion of the mortar joint to the clay unit surface with a look of genuine "earth-mortar". Preliminary tests with PNT-G penetrometer executed on several mortar joints in buildings n.16 (palazzo Sartoretti) n.18 (La Rocca) and n.23 (Casa di Cura, Cantone street) of table 4 confirmed that impression, furnishing values of compression strength included between 0,5-0,7 MPa.

After the surveys it was interesting to note that damages in Reggiolo city were generally higher than those of the surrounding municipalities located at shorter distance from the epicenter of the earthquake. Moreover, a simple estimation of local seismic intensity relating to PGA of accelerometer stations nearby provided an unsatisfactory result: measured PGA of about 0,05 g (as in the RAN station of Novellara) or values based only on attenuation laws, do not justify the high level of damages occurred in Reggiolo. Considering that the typology of the constructions is similar in the entire area, probably a significant amplification of the seismic motion occurred in Reggiolo. The causes of a possible local seismic amplification are not yet well recognized. Anyway, it is worthwhile to point out that most of the area was originally a marsh and only in recent centuries became a reclaimed land. In addition the geomorphology of the whole area of Reggiolo indicates a well defined levee ridge (height > 2 m, longitudinal slope < 1 ‰). Accurate (3rd level) micro-zonation analysis (ISSMGE 1999) is necessary in order to understand the causes (geotechnical or geomorphological conditions) of possible amplification effects observed in Reggiolo and to permit a proper restoration activity.

Table 4: Public buildings in Reggiolo (RE)

	Name	Position	Typology	n° floors	Ground area (m2)	Volume (m3)	Height (m)	Age	AEDES Agibility Index	MiBAC Damage Index
1	Centro Civico Medico Comunale	Isolated	Masonry	2	350	3200	9,00	1930	B	
2	Scuola d'infanzia Gioiosa	Isolated	Masonry	3	750	6975	3,20	1962/1971 and 1992/2001	A	
3	Scuola d'infanzia Bambi-Peter Pan	Isolated	R.C.	1	550	1710	3,20	1972/1981 e 2002	B	
4	Centro sociale polivalente	Extremity	R.C.	2	850	7750	12,00	>2002	B	
5	Bocciodromo Comunale	Extremity	R.C.	1	1000	5250	8,00	1972/1981	B	
6	Palestra sportiva Magnani	Isolated	R.C.	1	1100	5250	10,00	1992/2001	C	
7	Municipio	Extremity	R.C.	6	270	4500	19,00	1962/1971	E	
8	Scuola Media Carducci-Auditorium	Extremity	R.C.	4	350	1470	12,00	1992/2001	B	
9	Scuola Media Carducci-ed. principale	Extremity	Masonry	2	850	6600	10,00	<1919	E	0,63
10	Centro socio-sanitario edificio 32	Isolated	Masonry and R.C.	2	1100	6300	9,00	1919/1945 and 1962/1971	E	
11	Scuola elementare De Amicis- Ed. Principale	Extremity	R.C.	2	1450	8400	7,00	1962/1971	B	
12	Scuola elementare De Amicis- mensa	Extremity	R.C.	2	220	1140	7,00	>2002	C	
13	Scuola elementare De Amicis-palestra	Extremity	R.C.	1	600	2875	8,50	>2002	E	
14	Scuola d'infanzia Hansel e Gretel	Isolated	R.C.	1	250	1113	4,00	1972/1981 and 2002	C	
15	Scuola Materna Parrocchia Maria Immacolata	Isolated	Masonry	2	580	3450	7,50	1962/1971	A	
16	Palazzo Sartoretti	Extremity	Masonry	4	1020	13260	14,00	1800	E	0,60
17	Teatro Comunale Rinaldi	Isolated	Masonry	3	520	5150	5,80	1800	E	0,49
18	Rocca Comunale	Isolated	Masonry	2	1900	38000	4,00	1200	E	0,86
19	Cimitero Comunale	Isolated	R.C.	2	2470	17297	7,00	1930	C	0,10
20	Cimitero Villanova	Isolated	Masonry	1	130	1040	8,00	1950	E	0,37
21	Magazzino Comunale	Isolated	R.C.	1	480	2250	8,00	1972/1981	A	
22	Ex officina IPSIA Centro Sociale	Isolated	R.C.	1	220	600	4,00	1972/1981	B	
23	Casa di Riposo via Cantone	Isolated	Maosnry	2	700	5600	8,00	1920	E	

Palazzo Sartoretti – the Town Hall (the main façade)

The medieval “Rocca” (collapse events)

Casa di cura, Cantone street (view and PNT-G tests on mortar joints)

Municipal Theatre (the façade and the interior)

Fig. 36: historical masonry buildings in Reggiolo

 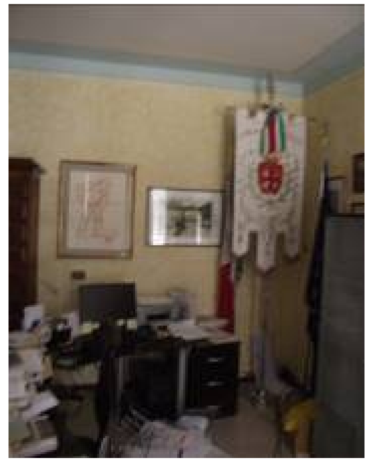

The new Town Hall (Martiri square)

The school De Amicis (XXV April street)

 

The sport hall De Amicis (XXV April street)

The Trentadue Building (Auditorium)

Fig.37: r.c..masonry infilled frames - public buildings in Reggiolo

Social Centre (view and tilting r.c. panels)

Sports hall Magnani – (general view and details of the weak supports)

The kindergarten Bambi-Peter Pan –(view and tilting r.c. panels)

Fig.38: r.c. prefabricated public buildings in Reggiolo

San Giovanni Battista Church – Concordia sulla Secchia

Santa Caterina Church – Concordia sulla Secchia

Cemetery of Carpi -

Fig. 39: historical religious buildings after earthquake

Fig. 40. View of prefabricated building with collapses on façade elements (Mirandola)

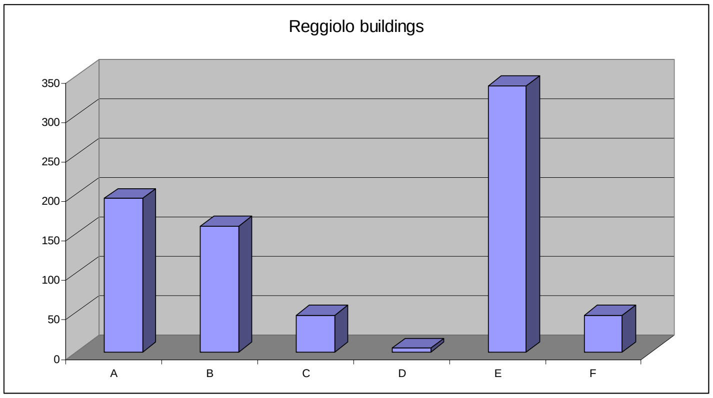

Fig. 41: distribution of AEDES Index in Reggiolo

In any case it was possible to perform an analysis on some failure mechanisms activated in the damaged masonry buildings of Reggiolo, by using the expressions provided by the italian codes (Circ. 617/2009) or by means of ITC-CNR CINE 1.0 code. As in (Andreini, De Falco & Sassu – 2012) each collapse mechanism achieves the role of "earthquake-sensor"; the values of PGA obtained in Reggiolo by equivalent static linear analysis are the following:

- Palazzo Sartoretti, the Town Hall – collapse of the corner - 0,16 g
- the medieval Rocca – collapse of a free wall – 0,12 g
- Casa di Cura, Cantone street – collapse of the façade – 0,13 g

From that values it is possible a first estimation of a high amplitude coefficient of the soil, comprised between 2,4 and 3,2.

The r.c. constructions – generally built after the 60s - have been affected mainly by damages for non-structural elements, especially in the external clay unit panels: the most frequent activated collapse mechanism consists in the out-of-plane tipping of the wall.

There were no observed striking collapse of r.c. precast structures, but it has become apparent vulnerability of public buildings, such as buildings No. 3 (the kindergarten Bambi-Peter Pan), No. 4 (Social Centre), No. 5 (Bowls Centre) and No. 6 (Sports hall): the incipient tilting of panels was opposed in some cases by thin metal bars, whose integrity is assured with narrow margin of safety the failure of substantial parts of the building.

A survey on private buildings of Reggiolo provides valuable insights about the level of damage estimated by AEDES forms and the speed with which citizenship has been active in initiating first repairs. Among about 800 buildings inspected, approximately 45% were accessible or repairable by means of emergency works, but more than 48% were completely unusable, which confirms the poor mechanical properties of the Reggiolo's soil, in relation to the intensity of seismic action from the epicenter. From the point of view of the age, it is observed that about a quarter of the buildings was built before 1945, two-thirds between 1945 and 1980 and 10% after 1980: in Reggiolo set of buildings there is a confirmation of the vulnerability of the constructions built in the period (50s-70s). Regarding the timeliness of consolidations in Reggiolo, in 25th of August 2012, 138 design post-earthquake reinforcements had already been presented, of which 45 related to manufacturing activities, indicating significant reactivity of the population.

Others structural situations.

Earthquake damages of the churches in Emilia are often relevant. As example in Fig. 39 the weak mortar used for the joints in clay units walls caused strong collapses of vaults, arches, façades, bell towers and walls. The circumstance of soft soil has probably increased the effects on the constructions.

Another interesting indicator is the direct experience gathered during site inspections: On May there were two shocks during the morning while many technicians were working to inspections, security safeguards and first reinforcements after the damage on 20th May. It has been possible to collect descriptions particularly effective: the ground showed visible vertical deformations typical of R-waves Rayleigh, measured in tens of centimeters (movement of cars and heavy flat on the floor to over a meter), as well as buildings - even those in masonry - translational and torsional displacements showed very large, in some cases not eligible in the calculations regulatory yet compatible with the balance of the building. The above observations lead to the following considerations: the first is that the jerky motions produced by surface R - waves may be important and under this circumstance the usual wave seismic isolators are totally ineffective. The second is that the legislation (NTC 2008) - in the case of global analyzes - is probably too harsh to the properties of masonry.

Many industrial buildings, however, experienced significant damage due to the collapse of non-structural elements: in some cases the panels have detached from the frames and plummeted to the foot rotation, leading to some as the collapse of the frame, in other cases the collapse panels or frames was induced by the earthquake instability of the racks, loaded with masses conspicuous, or other heavy equipment inside the building and not evaluated in the project. On occasion, there was also insufficient bearing capacity of prefabricated frames, as a result of the small rotation capacity of the connections, coupled with little or no hyperstatic structures. The attention of the designers, focused only on structural elements (beams, columns etc.), did not consider the dangerous influence of non-structural elements (i.e. precasted panels) or of the equipments inside the industrial buildings, causing strong damages as shown in the annexed photos; in this sense the lack of previous legislation and the lack of attention of the structural engineers to these aspects played a relevant role

CONCLUDING REMARKS

It is not possible to draw conclusions from an earthquake report but it is possible to point out the lesson learned. More specifically it is worthwhile to remark the following aspects:

- moderate earthquakes of May 20th and 29th 2012 have caused significative damages of both ancient and modern constructions;
- as far as the modern constructions are concerned the reasons of such a damages are essentially two:
    - untill 2010 the constructions were designed referring to the seismic zonation map of Figure 8 (i.e. in the territory under consideration till 2010 generally no seismic criterion was adopted for the new construction design, even though the seismic hazard map of Figure 9 had been known since 1999). It is necessary to explain that, according to Italian Legislation, the prescriptions of Building Codes are mandatory. Therefore, before 2010 there was no obligation to consider the hazard map of Figure 9 and after 2010 there was no obligation for retrofitting existing buildings (apart those considered as strategic for the Civil Service);
    - in the case of industrial buildings the effects of non – structural parts of the building on the construction structure were not considered in the design;
- as far as the ancient constructions are concerned the reasons of observed damages are essential due to the poor quality of the mortar and in the case of Reggiolo to some not yet well understood site effects.

As a main conclusion it is worthwhile to point out the need for a more effective divulgation of technical knowledge of a – seismic design of constructions and seismic risk among common people.

REFERENCES

Achenbach J.D. [1999]. *"Wave propagation in Elastic Solids*". North Holland, Amsterdam, Netherlands

Aki K. and P.G. Richards [1980]. *"Quantitative Seismology, Theory and Methods"*. Vol. 1-2 W.H.Freeman & Co., New York.

Ambraseys, N.N. [1988]. *"Engineering Seismology"*. Earthquake Engineering and Structural Dynamics, vol. 17, Elsevier, Amsterdam, pp. 1–105.

Anzidei M., Maramai A., Montone P. (Ed.s) [2012]. "*The Emilia (northern Italy) seismic sequence of May-June, 2012: preliminary data and results*", Annals of Geophysics, 55(4). doi:10.4401/ag-6114.

Arpa Emilia Romagna [2012], *http://telecontrollo.emiliacentrale.it/*

Balista, C., M. Calzolari, P. Campagnoli, A. Cardarelli, M. Cattani, V. Corazza, C. Corti, S. Gelichi, A. Gianferrari, N. Giordani, D. Labate, L. Malnati, R. Mussati, G. Pellacani, S. Pellegrini, R. Tarpini and C. Zanasi [2003]. *"Atlante dei Beni Archeologici della Provincia di Modena"*. Vol. I, Firenze, all'Insegna del Giglio.

Bindi, D., F. Pacor, L. Luzi, R. Puglia, M. Massa, G. Ameri and R. Paolucci [2011]. *"Ground motion prediction equations derived from the Italian strong motion database"*, Bulletin of Earthquake Engineering, 9, pp. 1899-1920; doi: 10.1007/

Boccaletti M., G. Corti and L. Martelli. [2011]. "Recent and active tectonics of the external zone of the Northern Apennines (Italy)", Int J Earth Sci (Geol Rundsch),100, pp. 1331–1348, DOI 10.1007/s00531-010-0545-y.

Boore, D. M. and J.J. Bommer [2005]. *"Processing of strong-motion accelerograms: Needs, options and consequences"*, Soil Dynamics and Earthquake Engineering, 25, pp. 93-115.

Caputo, R., Iordanidou, K., Minarelli, L., Papathanassiou, G., Poli, M., Rapti-Caputo, D., Sboras, S., Stefani, M., & Zanferrari, A. [2012]. Geological evidence of pre-2012 seismic events, Emilia-Romagna, Italy. Annals Of Geophysics, 55(4). doi:10.4401/ag-6148.

Castaldini D., M. Mazzucchelli and V. Pignatti [1992]. *"Geomorfologia e geochimica dei sedimenti del paleoalveo dei Barchessoni (San Martino Spino, bassa pianura modenese)"*, in: M. Calzolari and L. Malnati (eds.) *"Gli Etruschi nella Bassa Modenese"*, Gr. St. Bassa Modenese, pp. 207-224.

Castaldini, D. [1989a]. *"Evoluzione della rete idrografica centro padana in epoca protostorica e storica"*, in *Atti Conv. Naz. Studi Insediamenti e viabilità nell'alto ferrarese dall'Età Romana al Medioevo,* Cento 8-9 maggio 1987, Acc. delle Sc. di Ferrara, pp. 115-134.

Castaldini, D. [1989b]. "*Geomorfologia della bassa Pianura Padana modenese e dei territori limitrofi"*, in *"Mirandola e le valli, immagini e documenti"*, Tip. Golnelli, Mirandola, pp.25-37.

Castaldini, D. [1984]. *"Esempio di studio morfologico e geolitologico in un'area di pianura: il territorio del comune di Quistello (Provincia di Mantova)"*, Atti Soc. Nat. e Mat. di Modena, 115 , pp. 47-76.

Castaldini, D. and S. Raimondi [1985]. *"Geomorfologia dell' area di Pianura Padana compresa fra Cento, Finale Emilia e S. Agostino"*, Atti Soc. Nat. e Mat. di Modena, 116, pp. 147-176.

Castaldini, D., M. Mazzucchelli and V. Pignatti [1992]. *"Geomorfologia e geochimica dei sedimenti del paleoalveo dei Barchessoni (San Martino Spino, bassa pianura* *modenese)"*, in: M. Calzolari and L. Malnati (eds.), *Gli Etruschi nella Bassa Modenese*, Gruppo studi Bassa modenese, pp. 207-224.

Castaldini, D., M. Marchetti and A. Cardarelli [2009]. *"Geomorphological and archaeological aspects in the central Po Plain (Northern Italy)"*, in De Dapper M., Vermeulen F., Deprez, S. and Taelman D. (Editors), *Ol'man River.Geo-Archaeological aspects of rivers and river plains*, (ARGU 5), Universiteit Gent Academia Press, Belgium, pp. 193- 211.

Castelli, V., F. Bernardini, R. Camassi, C. Caracciolo, Castiglioni, G.B. Et Alii, [1997]. *"Carta geomorfologica della Pianura Padana alla scala 1:250.000"*, SELCA, Firenze.

Castiglioni, G.B. and G.B.Pellegrini [2001]. *"Illustrative Notes of the Geomorphological Map of Po Plain"*, Suppl. Geogr. Fis. Dinam. Quat., IV, pp. 1-208.

Crespellani, T., J. Facciorusso , A. Ghinelli, C. Madiai, S. Renzi and G. Vannucchi [2012]. *"Rapporto preliminare sui diffusi fenomeni di liquefazione verificatisi durante il terremoto in pianura padana emiliana del maggio 2012. 31 maggio 2012",* (Università degli Studi di Firenze, Dipartimento di Ingegneria Civile e Ambientale - sezione geotecnica), Technical report.

CSLP [2012] – updated version. http://www.cslp.it/ Spettri-NTCver.1.0.3.zip

Di Dio, G. [1998]. *"Riserve idriche sotterranee della Regione Emilia-Romagna"*. Technical report and six maps, 119 pp., Regione Emilia-Romagna – ENI AGIP, Bologna.

Di Manna, P., L. Guerrieri, L. Piccardi , E. Vittori, D. Castaldini ,A. Berlusconi, L. Bonadeo, V. Comerci, F. Ferrario, R. Gambillara, F. Livio, M. Lucarini and A.M. Michetti [2012], *"Ground effects induced by the 2012 seismic sequence in Emilia: implications for seismic hazard assessment in the Po Plain"*, Annals of Geophysics, 55(4), Special Issue "The Emilia seismic sequence of May-June, 2012: preliminary data and results". doi:10.4401/ag-6114. 697- 703..

Chioccarelli, E., F. De Luca and I. Iervolino [2012], *"Preliminary study of Emilia (May 20th 2012) earthquake ground motion records V2.1"*, available at www.reluis.it.

EC8 [2004], EN 1998-1:2004 Eurocode 8, *"Design of structures for earthquake resistance - Part 1: General rules, seismic actions and rules for buildings"*.

Ercolani, E. and L. Postpischl [2012], *"Looking for missing earthquake traces in the Ferrara-Modena plain: an update on historical seismicity"*, Annals Of Geophysics, 55(4), doi:10.4401/ag-6110.

Galli P., S. Castenetto, and E. Peronace [2012], *"The MCS macroseismic survey of the Emilia 2012 earthquakes"*, Annals Of Geophysics, 55(4), doi:10.4401/ag-6163.

Galli, P. [2000], *"New empirical relationships between magnitude and distance for liquefaction"*, Tectonophysics, 324, pp. 169–187.

Galli, P., S. Castenetto and E. Peronace [2012], *"May 2012 Emilia earthquakes (Mw 6, northern Italy): macroseismic effects distribution and seismotectonic implications"*, Alpine and Mediterranean Quaternary, 25 (2), pp. 105-123, in press, available online: http:/amq.aiqua.it.

Gorgoni, C, G. Martinelli and G.P. Sighinolfi G.P. [1982]. *"Stato termico e caratteri chimici delle acque sotterranee mediamente profonde della pianura emiliano-romagnola"*. In: Various Authors, *Caratteri geoidrologici e geotermici dell'Emilia-Romagna*, RER – CNR, MB T6, pp. 81-95, Pitagora Ed., Bologna.

Gruppo Lavoro Liquefazione [2012]. *"Primo rapporto sugli effetti della liquefazione osservati a S. Carlo, frazione di S. Agostino (Provincia di Ferrara)"*. A cura del gruppo di lavoro per la valutazione degli effetti di liquefazione a seguito dei terremoti del 20 e 29 maggio 2012 (Regione Emilia-Romagna, PG.2012.0134978 del 31/5/2012).

Guidoboni, E., G. Ferrari, D. Mariotti, A. Comastri, G. Tarabusi and G. Valensise [2007]. *"CFTI4Med, Catalogue of Strong Earthquakes in Italy (461 B.C.–1997) and Mediterranean Area (760 B.C.–1500)"*, INGV-SGA, available online: http://storing.ingv.it/cfti4med/.

Idriss, I.M., and R.W. Boulanger [2008]. *"Soil Liquefaction During Earthquakes"*, EERI Monograph.

INGV [2012] http://esse1-gis.mi.ingv.it/.

ISIDe Working Group INGV [2012] "*Italian Seismological Instrumental and parametric database*", http://iside.rm.ingv.it

ISSMGE [1999]. Technical Committee for Earthquake Geotechnical Engineering, TC4, ISSMGE "*Manual for Zonation on Seismic Geotechnical Hazards" (Revised Version)*. Tokyo, Japanese Geotechnical Society.

Kramer, S. [1996]. *"Geotechnical Earthquake Engineering"*. Prentice-Hall International Series, in: *Civil Engineering and Engineering Mechanics*.

Kuribayashi, E. and F.Tatsuoka [1975], *"Brief review of soil liquefaction during earthquakes in Japan"*, Soils and Foundations, Vol. 15, No. 4, pp. 81-92

Lai, C., F. Bozzoni, M.D. Mangriotis, M. Martinelli, L. Scandella and F. Decarro [2012], *"Geotechnical aspects of May 20th, 2012 M5.9 Emilia Earthquake, Italy"*, July 13 2012, EUCENTRE, Pavia, Italy.

Liu, Y. and J.F. Xie [1984]. *"Seismic liquefaction of sand"*, Earthquake Press, China (in Chinese).

Locati, M., R. Camassi and M. Stucchi [2011]. "DBMI11, the 2011 version of the Italian Macroseismic Database". Milano, Bologna, http://emidius.mi.ingv.it/DBMI11.

Lo Presti, D. C.F. and N. Squeglia [2011] *"Lesson learned from Liquefaction Potential Assessment of Silty Sand Deposits in a Case Study in Italy"*, Italian Geotechnical Journal, Vol. XLV, No. 2, pp. 68-79.

Marcaccio, M. and G. Martinelli [2012], *"Effects on the groundwater levels of the May-June 2012 Emilia seismic sequence"*, Annals Of Geophysics, 55(4). doi:10.4401/ag-6139, pp. 811-814

Montone, P., M. T. Mariucci, S. Pondrelli, and A. Amato [2004], *"An improved stress map for Italy and surrounding regions (central Mediterranean)"*, J. Geophys. Res., 109, B10410, doi:10.1029/2003JB002703.

Nakamura, Y. and M. Ueno [1986], *"A simple estimation method of dynamic characteristics of subsoil. Proceedings of the 7th Japan Earthquake Engineering Symposium"*, pp. 265-270 (in Japanese).

Ninfo, A., D. Zizioli, C. Meisina, D. Castaldini, F. Zucca, , L. Luzi and M. De Amicis [2012], *"The survey and mapping of sand-boil landforms related to the Emilia 2012 earthquakes: preliminary results"*. Annals Of Geophysics, 55(4). doi:10.4401/ag-6114, pp. 727-733

NTC [2008]. *"Nuove norme tecniche sulle costruzioni"*. DM 14 Gennaio. GU n°29, 04/02/2008.

Obermeier, S.E. [1996], *"Use of liquefaction induced features for paleoseismic analysis"*, Eng. Geol., pp. 44, 1-76.

Obermeier, S.F., S.M. Olson and .R.A. Green [2005], *"Field occurrences of liquefaction-induced features: a primer for engineering geologic analysis of paleoseismic shaking"*, Eng. Geol., 76, pp. 209–234.

Ori, G. G., and P. F. Friend [1984], *"Sedimentary basins formed and carried piggy- back on active thrust sheets"*, Geology, 12, pp. 475–478, doi:10.1130/0091- 7613

Pacor, F., R. Paolucci, G. Ameri, M. Massa, and R. Puglia [2011], *"Italian strong motion records in ITACA: overview and record processing"*, Bulletin of Earthquake Engineering, 9, pp. 1741-1759.

Pellegrini M. and A. Zavatti [1980]. *"Il sistema acquifero sotterraneo tra i fiumi Enza, Panaro e Po: alimentazione delle falde e scambi tra falde, correlazioni idrochimiche"*. Quaderni IRSA, 51(1), Roma.

Piccinini, D., N.A. Pino, and G. Saccorotti [2012], *"Source complexity of the May 20th, 2012, Mw=5.9 Ferrara (Italy) event"*, Annals Of Geophysics, 55(4).

Pieri M. and G. Groppi [1981]. *"Subsurface geological structure of the Po Plain (Italy)"*. C.N.R., Prog. Fin. Geodinamica, Pubbl. no. 414, pp. 1-13.

Pizzi A., Scisciani V. [2012]. *The May 2012 Emilia (Italy) earthquakes: preliminary interpretations on the seismogenic source and the origin of the coseismic ground effects.* Annals of Geophysics, 55(4), pp. 751- 757. doi:10.4401/ag-6114.

Pondrelli, S., S. Salimbeni, G. Ekström, A. Morelli, P. Gasperini, and G. Vannucci [2006], *"The Italian CMT dataset from 1977 to the present"*, Phys. Earth Planet. Int., 159(3–4), pp. 286–303, doi:10.1016/j.pepi.2006.07.008.

Prestininzi, A. and R.W. Romeo [2000], *"Earthquake-Induced Ground Failures in Italy"*, Eng. Geol., 58(3-4), pp. 387-397.

Regione Emilia-Romagna (Open file). La banca dati geognostica; http://ambiente.regione.emilia-romagna.it/geologia/cartografia/webgis-banchedati/banca-dati-geognostica

Rovida A., R. Camassi, P. Gasperini and M. Stucchi (eds.), [2011]. *"CPTI11, the 2011 version of the Parametric Catalogue of Italian Earthquakes"*. Milano, Bologna, http://emidius.mi.ingv.it/CPTI.

Scognamiglio, L., E. Tinti, and A. Michelini [2009], *"Real-time determination of seismic moment tensor for the Italian region"*, Bull. Seismol. Soc. Am., 99, 4, doi:10.1785/0120080104.

Vannucchi G., Crespellani T., Facciorusso J., Ghinelli A., Madiai C., Puliti A., Renzi S. [2012]. Soil liquefaction phenomena observed in recent seismic events in Emilia-Romagna Region, Italy. Ingegneria sismica, 26 Anno XXIX – N. 2-3, 20-30.

Wakamatsu K [1991]. *"Maps for historic liquefaction sites in Japan"*, Tokai University Press, Japan, 341 pp (in Japanese with English abstract).

Wakamatsu K. [1993]. *"History of soil liquefaction in Japan and assessment of liquefaction potential based on geomorphology"*. A Thesis in the Department of Architecture presented in partial fulfillment of the requirements for the Degree of Doctor of Engineering, Waseda University, Tokyo, Japan, 245 pp.

Youd, T.L., I.M Idriss, R.D. Andrus, I. Arango, C. Castro, J.T. Christian, R. Dobry, W.D.L. Finn, L.F. Harder, M.E. Hynes, K. Ishihara, J.P. Koester, S.C.C. Liao, W.F. Marcuson, G.R. Martin, J.K. Mitchell, Y. Moriwaku, M.S. Power, P.K.

Robertson, R.B. Seed. and, K.H. Stokoe [2001], *"Liquefaction Resistance of Soils. Summary Report from the 1996 NCEER and 1998 NCEER/NSF"*, Journal of Geotechnical and Geoenvironmental Engineering, ASCE, vol: 127 (10), pp. 817-833.

Zerbini, S., F. Matonti, and C. Doglioni [2006], *"Crustal movements in northeastern Italy from permanent GPS stations"*, Geophys. Res. Abstr., 8, Abstract 06257.